Gluon mass generation in the massless bound-state formalism

D. Ibañez[1] and J. Papavassiliou[1]

[1]*Department of Theoretical Physics and IFIC, University of Valencia and CSIC, E-46100, Valencia, Spain*

arXiv:1211.5314v1 [hep-ph] 22 Nov 2012

Abstract

We present a detailed, all-order study of gluon mass generation within the massless bound-state formalism, which constitutes the general framework for the systematic implementation of the Schwinger mechanism in non-Abelian gauge theories. The main ingredient of this formalism is the dynamical formation of bound-states with vanishing mass, which give rise to effective vertices containing massless poles; these latter vertices, in turn, trigger the Schwinger mechanism, and allow for the gauge-invariant generation of an effective gluon mass. This particular approach has the conceptual advantage of relating the gluon mass directly to quantities that are intrinsic to the bound-state formation itself, such as the "transition amplitude" and the corresponding "bound-state wave-function". As a result, the dynamical evolution of the gluon mass is largely determined by a Bethe-Salpeter equation that controls the dynamics of the relevant wave-function, rather than the Schwinger-Dyson equation of the gluon propagator, as happens in the standard treatment. The precise structure and field-theoretic properties of the transition amplitude are scrutinized in a variety of independent ways. In particular, a parallel study within the linear covariant (Landau) gauge and the background-field method reveals that a powerful identity, known to be valid at the level of conventional Green's functions, relates also the background and quantum transition amplitudes. Despite the differences in the ingredients and terminology employed, the massless bound-state formalism is absolutely equivalent to the standard approach based on Schwinger-Dyson equations. In fact, a set of powerful relations allow one to demonstrate the exact coincidence of the integral equations governing the momentum evolution of the gluon mass in both frameworks.

PACS numbers: 12.38.Aw, 12.38.Lg, 14.70.Dj

I. INTRODUCTION

The dynamical generation of an effective (momentum-dependent) gluon mass in pure Yang-Mills theories [1–3] (and eventually in QCD) has attracted considerable attention in recent years, because it furnishes a cogent theoretical explanation for a large number of important lattice findings [4–11]. This inherently nonperturbative phenomenon is usually studied within the formal machinery of the Schwinger-Dyson equations (SDEs), supplemented by a set of fundamental guiding principles, which enable the emergence of "massive" solutions, while preserving intact the gauge invariance of the theory [12, 13].

The main theoretical concept underlying the existence of such solutions is the Schwinger mechanism [14, 15]. The basic observation is that if the "vacuum polarization" acquires a pole at zero momentum transfer, then the vector meson becomes massive, even if the gauge symmetry forbids a mass at the level of the fundamental Lagrangian, as happens in the case of gauge theories. In the absence of elementary scalar fields, the origin of the aforementioned poles must be purely nonperturbative: for sufficiently strong binding, the mass of certain (colored) bound states may be reduced to zero [16–20]. In addition to triggering the Schwinger mechanism, these bound-state poles act as composite, longitudinally coupled Nambu-Goldstone bosons, enforcing the gauge invariance of the theory in the presence of gauge boson masses. Every such Goldstone-like scalar, "absorbed" by a gluon in order to acquire a mass, is expected to actually cancel out of the S-matrix against other massless poles or due to current conservation.

The concrete realization of the above general scenario in Yang-Mills theories proceeds by appealing to the existence of a special type of nonperturbative vertices, to be generically denoted by V (also referred to as "pole vertices"), which essentially transmit the effects of the composite excitations to the dynamical equations governing the various off-shell Green's functions. Specifically, the inclusion of these vertices (i) enables the SDE of the gluon propagator to admit massive solutions, and (ii) guarantees that the Ward identities (WIs) and the Slavnov-Taylor identities (STIs) of the theory maintain exactly the same form before and after gluon mass generation; a particular consequence of this important property is the exact transversality of the resulting (massive) gluon self-energy.

As has been demonstrated in a recent work [21], the full dynamical equation of the gluon mass in the Landau gauge may be derived from the SDE of the gluon propagator by

postulating the existence of the pole vertices, and employing the WIs and STIs they satisfy, together with their totally longitudinal nature (for related studies in the Coulomb gauge, see [22–25]). The resulting integral equation makes no reference to the closed form of these vertices, nor to the actual dynamical mechanism responsible for their existence. However, the details of the actual dynamical formation of the bound-state poles, and subsequently of the pole vertices, as well as their exact closed form, transcend the concrete purpose of obtaining a particular version of the gluon mass equation, and are of paramount importance for the self-consistency of the entire gluon mass generation scenario. In fact, it would be highly desirable to establish a precise quantitative connection between the fundamental ingredients composing these vertices and the gluon mass itself.

The purpose of the present work is to dissect the pole vertices and scrutinize the field-theoretic properties of their constituents, within the context of the "massless bound-state formalism", first introduced in some early seminal contributions to this subject [16–20], and further developed in [26]. The final outcome of this analysis is an alternative, but completely equivalent, description of the dynamical gluon mass in terms of quantities appearing naturally in the physics of bound states, such as the "transition amplitude" and the "bound-state wave function". This new description makes manifest some of the salient physical properties of the gluon mass (*e.g.*, positive-definiteness), and provides, in addition, a decisive confirmation of the self-consistency of the concepts and methodology employed.

Let us next present the general outline of the article, introducing some of the basic concepts, and commenting on the logical connections and delicate interplay between the various sections.

The starting point of our considerations is a brief review of the importance of the pole vertices for obtaining massive solutions out of the SDE for the gluon propagator, in a gauge invariant way, *i.e.*, preserving the form of the fundamental STIs of the theory (Section II).

Within the massless bound-state formalism, the pole vertices are composed of three fundamental ingredients. (i) The nonperturbative transition amplitude, to be denoted by $I(q^2)$, which connects a single gluon to the massless excitation. (ii) The scalar massless excitation, whose propagator furnishes the pole i/q^2, and (iii) a set of "proper vertex functions" [17] (or "bound-state wave functions"), to be generically denoted by B, (with appropriate Lorentz and color indices), which connect the massless excitation to a number of gluons and/or ghosts. The quantity $I(q^2)$ is universal, in the sense that it appears in all possible pole ver-

tices. Furthermore, it admits its own diagrammatic representation, which, in turn, involves the functions B. As a result, the dependence of the pole vertices on the Bs is quadratic (Section III).

When inserted into the SDE for the gluon propagator, and all diagrams are kept (no truncation), the special structure of the pole vertices allows one to obtain a very concise relation between the gluon mass and the square of the transition amplitude, given in Eq. (4.5). This relation demonstrates that, unless $I(q^2)$ vanishes identically, the gluon mass obtained is positive-definite (Section IV).

If the above construction is repeated within the combined framework of the pinch technique (PT) [1, 27–31] and the background field method (BFM) [32] (known as the "PT-BFM scheme" [33–35]), the relevant quantity to consider is the transition amplitude between a *background gluon* and the massless excitation, to be denoted by $\widetilde{I}(q^2)$ (all other ingredients remain identical). The mass of the propagator connecting a background (B) and a quantum gluon (Q) can then be expressed as the product of $I(q^2)$ and $\widetilde{I}(q^2)$; an equivalent relation may also be obtained from the background-background propagator (BB). The additional fact that the PT-BFM gluon propagators (QB and BB) are related to the conventional one (QQ) by a set of powerful identities (known as Background-Quantum identities (BQIs) [36, 37]), allows one finally to relate $I(q^2)$ and $\widetilde{I}(q^2)$ as shown in Eq. (5.12) (Section V).

Evidently, Eq. (5.12) has emerged as a self-consistency requirement between two different formulations of the SDEs (conventional and PT-BFM), which, in their untruncated version, must furnish the same physics. It would be very important, however, to establish the validity of Eq. (5.12) in a more direct, explicit way, by operating at the level of the pole vertices themselves, where $I(q^2)$ and $\widetilde{I}(q^2)$ make their primary appearance. To that end, we will carry out the explicit construction of the three-gluon pole vertex, both in the conventional and the BFM formalism, using as a sole input the WI and/or STIs they satisfy, and their totally longitudinal nature (subsection VI A). The comparison of the two, after judicious identification of the parts that contribute to the gluon mass equation, reproduces precisely Eq. (5.12) (subsection VI B).

It turns out that an even more fundamental derivation of Eq. (5.12) may be devised, which takes one back to the underpinnings of the PT-BFM connection: the BQIs, which are formally obtained within the Batalin-Vilkovisky (BV) formalism [38, 39], can be alternatively derived through the diagrammatic rearrangements implemented by the PT (Section VII). In

the case of the SDE series containing regular (fully dressed) vertices, such a diagrammatic derivation amounts finally to the demonstration of the nonperturbative PT-BFM equivalence [35]. From the operational point of view, the standard PT construction boils down to the judicious exploitation of the rearrangements produced when certain longitudinal (pinching) momenta trigger the STIs satisfied by the aforementioned vertices; the required STIs are known from the formal machinery of the BV, or alternative formalisms. A priori, the implementation of this procedure at the level of the diagrammatic representation of the $I(q^2)$ is thwarted by the fact that the pinching momenta will act on the B vertices (introduced above), whose STIs, however, are not formally known. Nonetheless, the explicit construction of the pole vertex, and the subsequent line of reasoning, furnish precisely the missing STI, and make the PT-driven diagrammatic construction possible (subsection VII A). An interesting by-product of this construction is the derivation of an integral constraint between the B-vertex functions containing ghost legs. When combined with the recent lattice findings on the infrared behavior of the ghost propagator, this constraint strongly suggests the individual vanishing of all such ghost vertex functions (subsection VII B).

The diagrammatic evaluation of the transition amplitude furnishes Eq. (8.15), which expresses this fundamental ingredient of the bound-state formalism in terms of a double integral containing solely the vertex $B_{\mu\nu}$. Even though this vertex function is not known for general momenta, the powerful relation of Eq. (8.18), first derived in [26], relates its $g_{\mu\nu}$ form factor to the gluon mass. This relation, in turn, allows one to recover the mass equation derived in [21], following a completely different methodology and formalism. The resulting exact coincidence reveals an impressive complementarity between two formally distinct methods (subsection VIII A).

The equivalence of the two formalisms established in the previous subsection is exact only when no approximations are employed in either one. However, in practice approximations must be carried out, and as a result, in general, due to the difference of the intermediate steps, a modified momentum dependence for the gluon masses will be obtained. In subsection VIII B we outline the general computational procedure that must be followed within the massless bound-state formalism in order to determine the dynamical gluon mass. The nature of this procedure is *a-priori* dissimilar to that employed in [21]; thus, whereas an SDE equation is solved in the latter case, now the main dynamical ingredient is the Bethe-Salpeter equation (BSE) that controls the evolution of the relevant bound-state wave function. In

the qualitative discussion presented here, we focus on the difference in the momentum-dependence of the gluon mass that one observes at the lowest level of approximation within both formalisms.

Finally, our conclusions and discussion are presented in Section IX .

II. GETTING MASSIVE SOLUTIONS FROM THE GLUON SDE

In this section we review the general principles that allow the generation of massive solutions out of the gluon SDE, and study in detail the general structure of the special pole vertices that trigger this effect (for different approaches, see, *e.g.*, [40–55]).

A. General principles

The full gluon propagator $\Delta^{ab}_{\mu\nu}(q) = \delta^{ab}\Delta_{\mu\nu}(q)$ in the Landau gauge is defined as

$$\Delta_{\mu\nu}(q) = -iP_{\mu\nu}(q)\Delta(q^2)\,, \tag{2.1}$$

where

$$P_{\mu\nu}(q) = g_{\mu\nu} - \frac{q_\mu q_\nu}{q^2}\,, \tag{2.2}$$

is the usual transverse projector, and the scalar cofactor $\Delta(q^2)$ is related to the (all-order) gluon self-energy $\Pi_{\mu\nu}(q) = P_{\mu\nu}(q)\Pi(q^2)$ through

$$\Delta^{-1}(q^2) = q^2 + i\Pi(q^2). \tag{2.3}$$

Alternatively, one may introduce the *inverse* of the gluon dressing function, $J(q^2)$, defined as [56]

$$\Delta^{-1}(q^2) = q^2 J(q^2)\,. \tag{2.4}$$

Let us consider the SDE for the gluon propagator in the conventional formulation of Yang-Mills (*i.e.*, linear R_ξ gauges)

$$\Delta^{-1}(q^2)P_{\mu\nu}(q) = q^2 P_{\mu\nu}(q) + i\Pi_{\mu\nu}(q), \tag{2.5}$$

with the self-energy given by

$$\Pi_{\mu\nu}(q) = \sum_{i=1}^{5}(a_i)_{\mu\nu}\,, \tag{2.6}$$

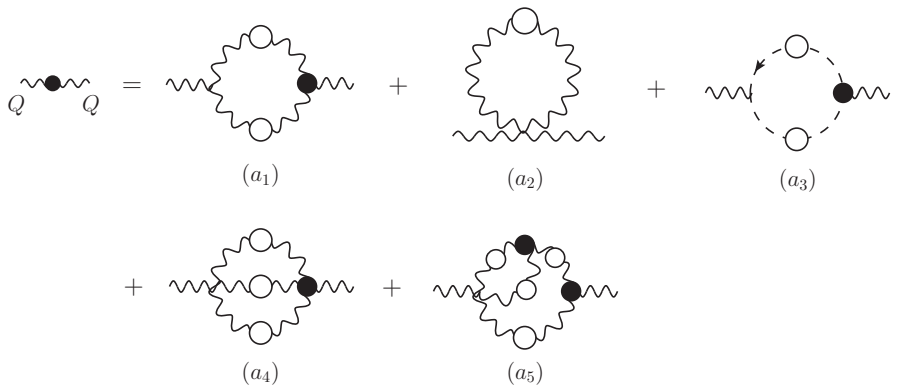

FIG. 1: SDE satisfied by the conventional gluon self-energy, with two quantum gluons (Q) entering. White (black) circles denote fully-dressed propagators (vertices).

where the diagrams (a_i) are shown in Fig. 1. Note that the full (untruncated) self-energy is transverse, namely

$$q^\mu \Pi_{\mu\nu}(q) = \sum_{i=1}^{5} q^\mu (a_i)_{\mu\nu} = 0\,. \tag{2.7}$$

It turns out that, with the Schwinger mechanism turned off (*i.e.*, in the absence of massless poles in the vertices) the SDE leads to the conclusion that $\Delta^{-1}(0) = 0$, namely the absence of massive solutions.

In order to obtain massive solutions out of the above SDE, and preserve, at the same time, the gauge invariance intact, one must carry out the crucial substitution

$$\Gamma \longmapsto \Gamma' = \Gamma_m + V, \tag{2.8}$$

to all fully-dressed interaction vertices appearing in Eq. (2.5). The main characteristic of the vertices V, which sharply differentiates them from ordinary vertex contributions, is that they contain massless poles, originating from the contributions of bound-state excitations. Such dynamically generated poles are to be clearly distinguished from poles related to ordinary massless propagators, associated with elementary fields in the original Lagrangian. In addition, they are completely *longitudinally* coupled, *i.e.*, they satisfy conditions of the type (for the case of the three-gluon vertex)

$$P^{\alpha'\alpha}(q) P^{\mu'\mu}(r) P^{\nu'\nu}(p) V_{\alpha'\mu'\nu'}(q,r,p) = 0. \tag{2.9}$$

As for the vertices Γ_m, they are given by the same graphs as the Γ before, but with gluon propagators replaced by massive ones [see Eq. (2.12)], implementing simultaneously Eq. (2.8).

The new (massive) self-energy is then given by

$$\Pi_{\mu\nu}(q) = \sum_{i=1}^{5} (a_i')_{\mu\nu}, \tag{2.10}$$

where the "prime" indicates that the various fully-dressed vertices appearing inside the corresponding diagrams of the gluon self-energy have been replaced by their primed counterparts, as in Eq. (2.8). It is important to emphasize that, since the above replacement maintains the STIs of the theory unaltered, the transversality of the massive self-energy persists, *i.e.*,

$$\sum_{i=1}^{5} q^{\mu} (a_i')_{\mu\nu} = 0\,. \tag{2.11}$$

The appearance of massive solutions amounts effectively to the change (in Minkowski space)

$$\Delta^{-1}(q^2) = q^2 J(q^2) \longmapsto \Delta_m^{-1}(q^2) = q^2 J_m(q^2) - m^2(q^2), \tag{2.12}$$

with $m^2(0) \neq 0$ (of course, in Euclidean space, one must find $\Delta_m^{-1}(0) > 0$). The subscript "m" in J_m indicates that effectively one has now a mass inside the various expressions: for example, whereas perturbatively $J(q^2) \sim \ln q^2$, after dynamical gluon mass generation has taken place, one has $J_m(q^2) \sim \ln(q^2 + m^2)$.

The actual evaluation of the relevant diagrams may be carried out by appealing to the basic global features of the V vertices, as deduced from the STIs and their complete longitudinality [21]. The final upshot is that the SDE may be schematically cast into the form (Minkowski space)

$$q^2 J_m(q^2) - m^2(q^2) = q^2 \left[1 + \mathcal{K}_1(q^2, m^2, \Delta_m)\right] + \mathcal{K}_2(q^2, m^2, \Delta_m), \tag{2.13}$$

such that $q^2 \mathcal{K}_1(q^2, m^2, \Delta_m) \to 0$, as $q^2 \to 0$, whereas $\mathcal{K}_2(q^2, m^2, \Delta_m) \neq 0$ in the same limit, precisely because it includes the term $1/q^2$ contained inside $V_{\alpha\mu\nu}(q, r, p)$. This form, in turn, gives rise to two coupled integral equations, an inhomogeneous equation for $J_m(q^2)$, and a homogeneous one for $m^2(q^2)$ (the latter is usually referred to as the "mass equation"), of the generic type

$$J_m(q^2) \;=\; 1 + \int_k \mathcal{K}_1(q^2, m^2, \Delta_m), \tag{2.14}$$

$$m^2(q^2) \;=\; -\int_k \mathcal{K}_2(q^2, m^2, \Delta_m). \tag{2.15}$$

Physically meaningful (*i.e.*, positive definite and monotonically decreasing) solutions to an approximate version of the full mass equation have been recently presented in [21].

B. Structure of the vertices V

We will next consider the decomposition of the vertices V that emerges in a natural way, if one employs as a criterion the effect that the various components of V may have on the gluon SDE. For concreteness we will focus on the case $V_{\alpha\mu\nu}$; however, all basic arguments may be straightforwardly extended to any vertex of the type V.

Since the main function of the vertex $V_{\alpha\mu\nu}$ is to generate a mass term when inserted into the graph (a_1) of Fig. 1, it must contain components that do not vanish as $q \to 0$. To study this point in more detail, we first separate V into two distinct parts, namely

$$V_{\alpha\mu\nu}(q,r,p) = U_{\alpha\mu\nu}(q,r,p) + R_{\alpha\mu\nu}(q,r,p)\,, \tag{2.16}$$

defined as follows. U is the part of V that has its Lorentz index α saturated by the momentum q; thus, it contains necessarily the explicit q-channel massless excitation, namely the $1/q^2$ poles. It assumes the general form

$$U_{\alpha\mu\nu}(q,r,p) = \frac{q_\alpha}{q^2} C_{\mu\nu}(q,r,p), \tag{2.17}$$

where, due to Bose symmetry under the exchange $r \leftrightarrow p$, $\mu \leftrightarrow \nu$, $C_{\mu\nu}(q,r,p)$ must satisfy $C_{\nu\mu}(q,p,r) = -C_{\mu\nu}(q,r,p)$; as a result, $C_{\mu\nu}(0,-p,p) = 0$.

The term R contains everything else; in particular, the massless excitations in the other two kinematic channels, namely $1/r^2$ and $1/p^2$ (but not $1/q^2$) are assigned to R. Thus, for example, terms of the form $q_\alpha g_{\mu\nu}$ and $q_\alpha r_\mu p_\nu$ are assigned to $U_{\alpha\mu\nu}$, while terms of the type $p_\nu g_{\alpha\mu}$ and $r_\mu g_{\alpha\nu}$ belong to R. Evidently, $P^{\mu'\mu}(r)P^{\nu'\nu}(p)R_{\alpha\mu'\nu'}(q,r,p) = 0$. In addition, again due to Bose symmetry, we have that $R_{\alpha\mu\nu}(0,-p,p) = 0$.

Consider now the individual effect that U and R have when inserted into the gluon SDE, specifically the graph (a_1) of Fig. 1. Of course, it is expected, on general grounds, that R should not generate mass terms, because it does not contain poles of the type $1/q^2$; this is indeed what happens. If we work in the Landau gauge, any contribution from R vanishes for a simple kinematic reason, namely the above transversality condition satisfied by R. Away from the Landau gauge, R does not contribute to the mass equation Eq. (2.15) either, because $R_{\alpha\mu\nu}(0,-p,p) = 0$ and there is no $1/q^2$ term that could compensate this. Thus, R seems to contributes, in a natural way, to the equation for $J_m(q^2)$.

In fact, it is relatively straightforward to establish that, in the limit $q \to 0$, the SDE contribution generated by R vanishes as $\mathcal{O}(q^2)$ (or faster). Indeed, let us set $p = k$, the

virtual integration momentum in the SDE diagram; given that $R_{\alpha\mu\nu}(0,-k,k)=0$, a Taylor expansion of R around $q^2=0$ gives (suppressing indices)

$$R(q,-q-k,k)=2(qk)R'(k^2)+\mathcal{O}(q^2)\,. \tag{2.18}$$

Now, the first term is odd in k, and therefore the corresponding integral vanishes. As a result, the term $2(qk)R'(k^2)$ must be multiplied by another term proportional to (qk), coming from the rest of the terms (propagators, vertices, etc) appearing in the integrand. Thus, the resulting contribution is of order $\mathcal{O}(q^2)$ (or higher), as announced. The importance of this property is related to the fact that, in order to arrive at Eq. (2.14), one must pull out of the corresponding integral equation a factor of q^2; had the integrand vanished slower than $\mathcal{O}(q^2)$, one would get a divergent contribution for $J_m(0)$, which would be physically unacceptable, given that $J_m(0)$ is inversely proportional to the infrared finite QCD effective charge [see, *e.g.*, [57], and references therein].

Therefore, the only term that can contribute to the gluon mass equation is $U_{\alpha\mu\nu}(q,r,p)$; the precise contribution will depend, of course, on the exact form and behaviour of the cofactor $C_{\mu\nu}(q,r,p)$, as $q\to 0$. It is clear for instance, that if $C_{\mu\nu}(q,r,p)$ contains terms that behave as $\mathcal{O}(q^{1+c})$, with $c>0$, as $q\to 0$, then these terms could not possibly trigger the Schwinger mechanism, because the effect of the pole would be counteracted by the positive powers of q. On the other hand, terms that vanish as $\mathcal{O}(q^{1-c})$, would give rise to divergent results; however, this latter possibility does not occur, again due to the Bose symmetry of V with respect to $p\leftrightarrow r$. Thus, the only terms of $C_{\mu\nu}$ relevant for gluon mass generation are those that vanish as $\mathcal{O}(q)$ ($c=0$).

These observations motivate the separation of $U_{\alpha\mu\nu}(q,r,p)$ into two parts, one that behaves as a constant, $\mathcal{O}(q^0)$, thus contributing to the mass equation (to be denoted by $\mathcal{U}_{\alpha\mu\nu}$), and one that vanishes as $\mathcal{O}(q^c)$, $c>0$, and can be naturally reassigned to R (to be denoted by $\mathcal{U}'_{\alpha\mu\nu}$). In fact, due to the same reason explained above, namely, the absence of divergent contributions at the level of Eq. (2.14), we must have that $c\geq 1$; actually, the explicit construction presented in Section VI [*e.g.* Eq. (6.24) and ensuing discussion], reveals that $c=1$. Thus,

$$U_{\alpha\mu\nu}(q,r,p)=\underbrace{\mathcal{U}_{\alpha\mu\nu}(q,r,p)}_{\mathcal{O}(q^0)}+\underbrace{\mathcal{U}'_{\alpha\mu\nu}(q,r,p)}_{\mathcal{O}(q)} \tag{2.19}$$

Then, setting

$$\mathcal{R}_{\alpha\mu\nu}(q,r,p) = R_{\alpha\mu\nu}(q,r,p) + \mathcal{U}'_{\alpha\mu\nu}(q,r,p) \tag{2.20}$$

we arrive at the final separation

$$V_{\alpha\mu\nu}(q,r,p) = \underbrace{\mathcal{U}_{\alpha\mu\nu}(q,r,p)}_{m^2(q^2)} + \underbrace{\mathcal{R}_{\alpha\mu\nu}(q,r,p)}_{J_m(q^2)} \tag{2.21}$$

where the curly brackets below each term indicate to which equation [Eq. (2.14) or Eq. (2.15)] each term will contribute.

III. MASSLESS BOUND-STATE FORMALISM

Whereas in the SDE approach outlined in the previous section one relies predominantly on the global properties of the vertices V, within the massless bound-state formalism one takes, instead, a closer look at the field-theoretic composition of these vertices, establishing fundamental relations between their internal ingredients and the gluon mass. This becomes possible thanks to the key observation that, since the fully dressed vertices appearing in the diagrams of Fig. 1 are themselves governed by their own SDEs, the appearance of such massless poles must be associated with very concrete modifications in the various structures composing them.

Let us begin by recalling that, in general, when setting up the usual SDE for any fully-dressed vertex contained in Eq. (2.5), a particular field (leg) is singled out, and is connected to the various multiparticle kernels through all elementary vertices of the theory involving this field (leg). The remaining legs enter into the various diagrams through the aforemen-

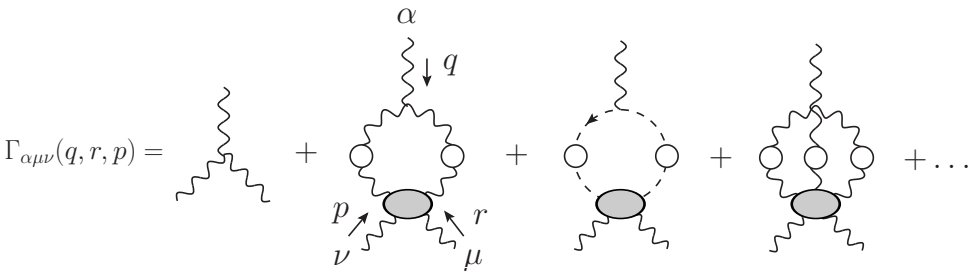

FIG. 2: The SDE for the Q^3 vertex $\Gamma_{\alpha\mu\nu}(q,r,p)$. Gray blobs denote the conventional 1PI (with respect to vertical cuts) multiparticle kernels.

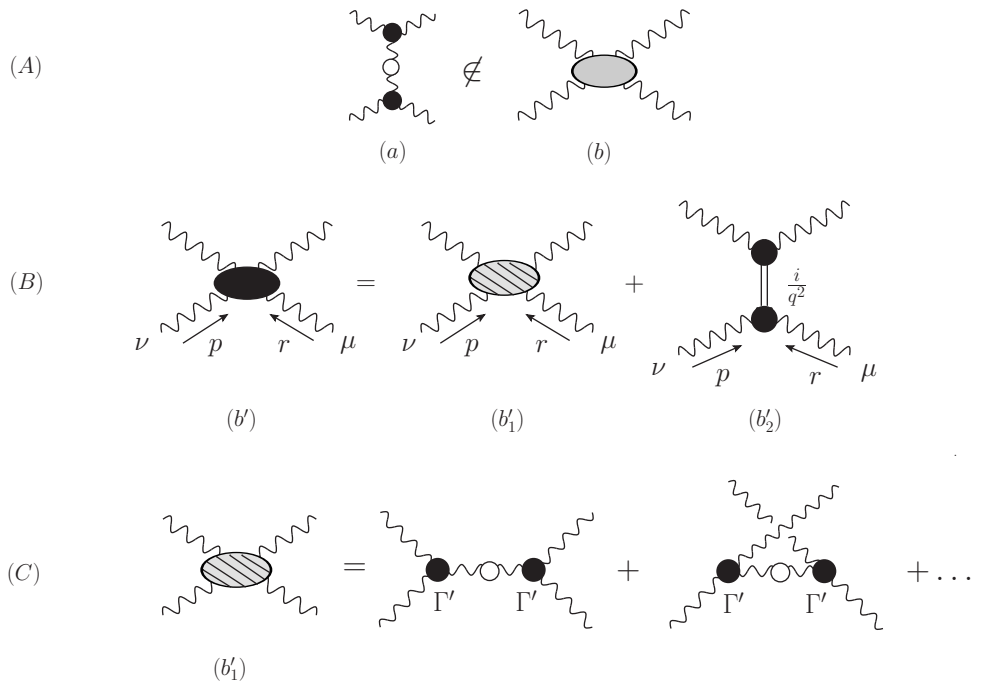

FIG. 3: (A) A diagram not included into the standard kernel. (B) The kernel with the Schwinger mechanism turned on: in addition to the "regular part" (b'_1) (gray striated), the massless excitation in the q-channel (b'_2) is added. (C) The part (b'_1) is obtained from the original (gray) kernel (b) by inserting massive gluon propagators into its diagrams, and carrying out the substitution Eq. (2.8) in the fully-dressed vertices of the skeleton expansion.

tioned multiparticle kernels, or, in terms of the standard skeleton expansions, through fully-dressed vertices (instead of tree-level ones). For example, in the case of the Q^3 three-gluon vertex $\Gamma_{\alpha\mu\nu}(q,r,p)$ we have (with a certain hindsight) identified the special leg to be the one entering into graph (a_1) of Fig. 1 from the right, carrying momentum q; the corresponding vertex SDE is shown in Fig. 2.

Now, when the Schwinger mechanism is turned off, the various multiparticle kernels appearing in the SDE for the Q^3 vertex have a complicated skeleton expansion, but their common characteristic is that they are *one-particle irreducible* with respect to cuts in the direction of the momentum q. Thus, for example, diagram (a) of Fig. 3 is explicitly excluded from the (gray) four-gluon kernel (b), and the same is true for all other kernels.

When the Schwinger mechanism is turned on, the structure of the kernels is modified by the presence of the composite massless excitations, described by a propagator of the type i/q^2. For example, as shown in Fig. 3, the gray four-gluon kernel is converted into a black

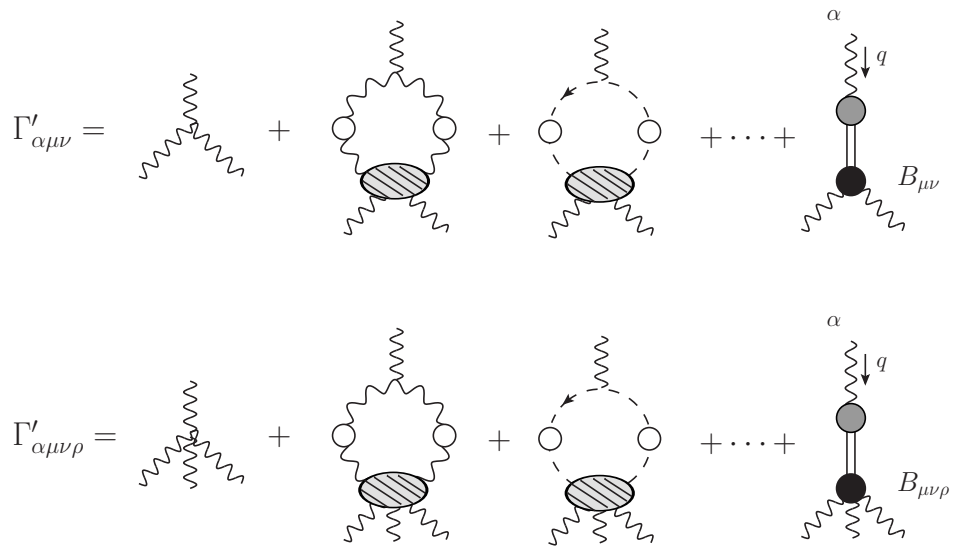

FIG. 4: The SDEs for the full three and four gluon vertices in the presence of their pole parts. Note that (i) the new SDE kernels are modified with respect to those appearing in Fig. 2; (ii) the last term in these SDEs corresponds to the $\mathcal{U}$ part of the pole vertices.

kernel, diagram (b'), which is the sum of two parts: (i) the term (b'_1), which corresponds to a kernel (gray striated) that is "regular" with respect to the q-channel, and (ii) the term (b'_2), which describes the exchange of the composite massless excitation between two gluons in the q-channel.

Thus, when the replacements of Eq. (2.12) and Eq. (2.8) are carried out, the SDE for the different interaction vertices in the presence of their pole parts will be given by expansions such as those shown in Fig. 4.

These modifications in the composition of the kernels give rise precisely to the vertices V mentioned earlier. A closer look at the structure of the terms comprising the last term in Fig. 4 reveals that the Lorentz index α (of the leg carrying the momentum q) is saturated precisely by the momentum q. Similarly, Bose symmetry forces the same behavior on the other two channels, so that, in the end, we obtain a totally longitudinal structure, *i.e.*, Eq. (2.9).

At this point it is advantageous to make the nonperturbative pole manifest, and cast the last term of the three-gluon vertex in the form of Fig. 4, by setting

$$\mathcal{U}_{\alpha\mu\nu}(q,r,p) = I_\alpha(q)\frac{i}{q^2}B_{\mu\nu}(q,r,p)\,; \tag{3.1}$$

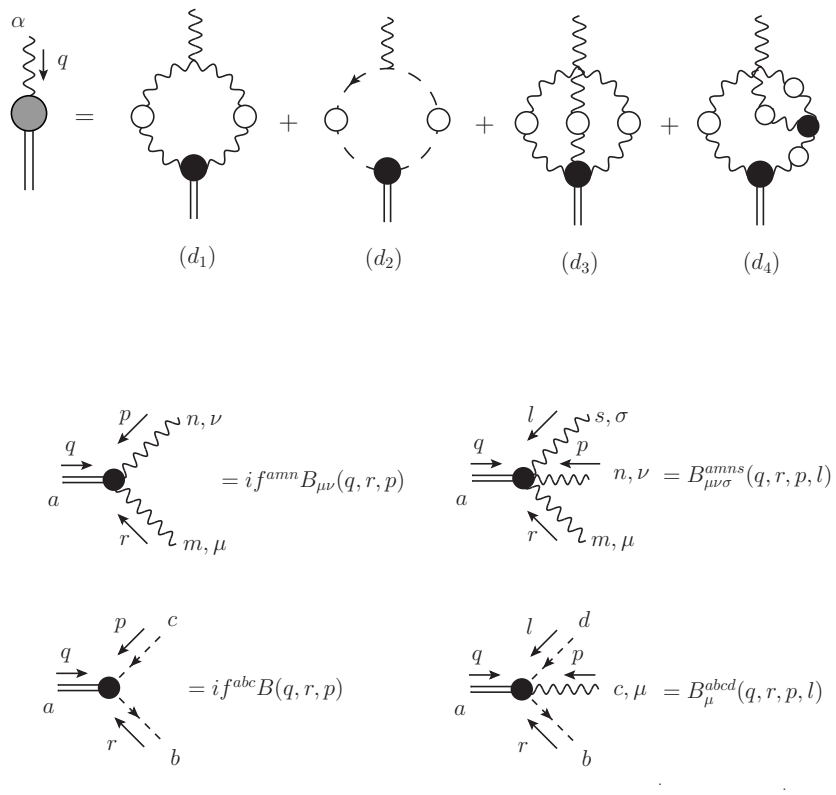

FIG. 5: Diagrammatic representation of the transition amplitude $I_\alpha(q)$, and the Feynman rules for the different effective vertices B.

$I_\alpha(q)$ denotes the transition amplitude that mixes a quantum gluon with the massless excitation, i/q^2 corresponds to the propagator of the massless excitation, and B is an effective vertex describing the interaction between the massless excitation and gluons and/or ghosts. In the standard language used in bound-state physics, B represents the "bound-state wave function" (or "Bethe-Salpeter wave function"). Clearly, due to Lorentz invariance,

$$I_\alpha(q) = q_\alpha I(q^2), \tag{3.2}$$

and the scalar cofactor, to be referred as the "transition function", is simply given by

$$I(q^2) = \frac{q^\alpha}{q^2} I_\alpha(q). \tag{3.3}$$

Furthermore, notice that the transition amplitude $I_\alpha(q)$ is universal, in the sense that it constitutes a common ingredient of all V vertices, namely

$$\mathcal{U}_{\alpha\{\dots\}}(q,\dots) = I_\alpha(q)\frac{i}{q^2}B_{\{\dots\}}(q,\dots); \tag{3.4}$$

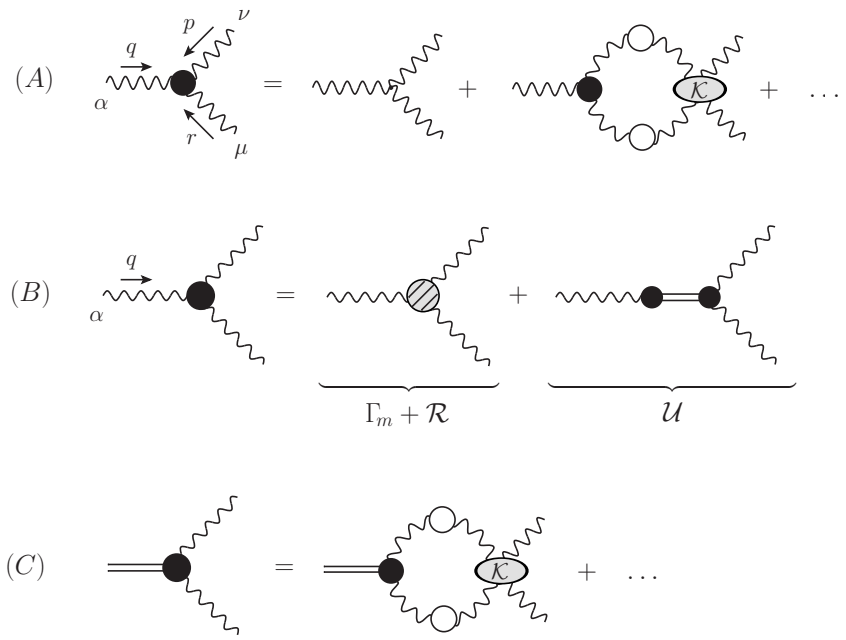

FIG. 6: Basic steps in the derivation of the BSEs that govern the dynamics of the effective vertices B.

thus, the difference between the various $\mathcal{U}_{\alpha\{\dots\}}$ vertices is solely encoded into the structure of the wave functions $B_{\{\dots\}}$. The diagrammatic representation of the transition amplitude as well as the different effective vertices B are shown in Fig. 5. It is important to recognize that the $\mathcal{U}_{\alpha\{\dots\}}$ depend *quadratically* on the $B_{\{\dots\}}$, since $I_\alpha(q)$ depends linearly on them.

As has been explained in the literature, the dynamics of the B functions may be determined, at least in principle, from a set of homogeneous (coupled and nonlinear) integral equations, known as BSEs. This particular set of equations must admit nontrivial solutions, which, when properly adapted to the kinematic details of the problem at hand, will furnish the momentum dependence of the wave functions B.

The way to obtain this set of equations is by first rearranging the vertex SDE in such a way as to replace the bare vertex appearing in the original expansion (*e.g.*, Fig. 2) by a fully dressed one (Fig. 6, line A). At the same time, and as a consequence of this rearrangement, one must replace the standard SD kernel by the corresponding Bethe-Salpeter kernel (denoted by $\mathcal{K}$ in Fig. 6); the two kernels are diagrammatically different, and are formally related by a standard all-order formula [58–60]. The next step is to separate the full vertex into the "regular" part, namely the part that behaves as a regular function in the limit

$q \to 0$, and the pole part, $1/q^2$, as shown in Fig. 6, line B. Note that the full regular part is the sum of Γ_m and the term $\mathcal{R}$ coming from V, since neither of these two terms diverges in the aforementioned limit. Then, this separation is carried out on both sides of the equation; since the vertex on the right-hand side (rhs) is now fully dressed, it too possesses a pole $1/q^2$. The final dynamical equation for B emerges by equating the coefficients multiplying the pole term on both sides, as seen in Fig. 6, line C. In the same way, the dynamical equation for the regular part is given by the remaining terms.

IV. RELATING THE GLUON MASS WITH THE TRANSITION AMPLITUDE

The aim of this section is to derive the fundamental formula that relates the effective gluon mass with the square of the transition amplitude.

To that end, let us go back to the SDE for the gluon propagator with the replacements given in Eqs.(2.8)-(2.12) already implemented, namely (Landau gauge)

$$[q^2 J_m(q^2) - m^2(q^2)]P_{\mu\nu}(q) = q^2 P_{\mu\nu}(q) + i\sum_{i=1}^{5}(a_i')_{\mu\nu}, \tag{4.1}$$

It turns out that the most expeditious way for deriving the gluon mass equation, and from it the desired relation between $m^2(q^2)$ and $I(q^2)$, is to identify, on both sides of Eq. (4.1), the cofactors of the tensorial structure $q_\mu q_\nu/q^2$ that survive the limit $q^2 \to 0$, and then set them equal to each other. In doing so, it is clear that the left-hand side (lhs) of Eq. (4.1) furnishes simply

$$[\text{lhs}]_{\mu\nu} = \frac{q_\mu q_\nu}{q^2} m^2(q^2). \tag{4.2}$$

On the other hand, the corresponding contribution from the rhs is directly related to the $\mathcal{U}$ part of the V vertices (see discussion in subsection II B), which, due to their very definition [see Eq. (3.4)], are all proportional to q_ν.

The procedure described above is exemplified in Fig. 7 for the particular case of the diagram (a_1'). Specifically, in the first step one separates the regular part Γ_m from the pole part V of the full Q^3 vertex Γ'. In the second step the pole part V is written as the sum of the $\mathcal{U}$ part (containing the explicit q-channel massless excitation) and the $\mathcal{R}$ part. Finally, due to the special structure of the $\mathcal{U}$ part, this contribution is proportional to $q_\mu q_\nu/q^2$, and contributes to the rhs of the mass equation.

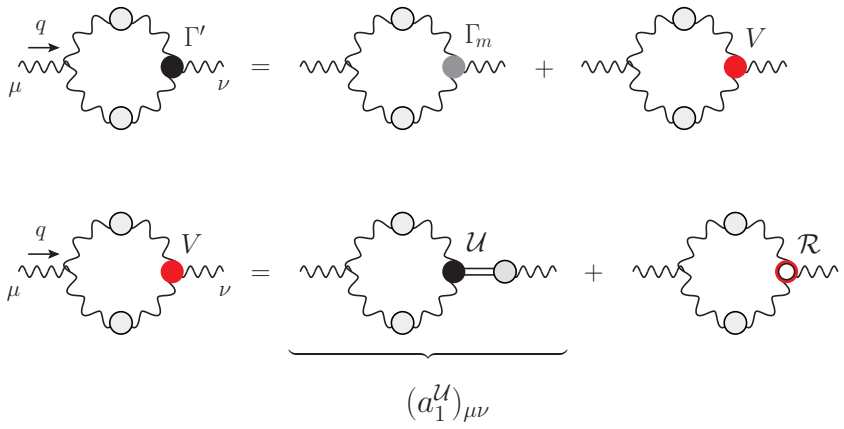

FIG. 7: Procedure for isolating the contribution of diagram (a_1') to the gluon mass equation.

The next step is to carry out this procedure to the $\mathcal{U}$ parts of all diagrams, and determine the complete contribution to the rhs of the mass equation, as shown pictorially in Fig. 8. It is clear that from all diagrams containing the $\mathcal{U}$ parts (first line of Fig. 8) one may factor out the common quantity $I(q^2)$, since, as we have emphasized in the previous section, $I(q^2)$ is universal (second line of Fig. 8). Then, quite interestingly, the sum of the terms in the parenthesis is nothing else than the diagrammatic representation of $I(q^2)$, given in Fig. 5 (note that all combinatorial factors work out exactly).

So, applying this procedure for each one of the fully-dressed vertices appearing in the SDE Eq. (4.1), one can put together the contributions of the several $\mathcal{U}$ parts to the gluon self-energy, as shown in Fig. 8,

$$\sum_{i=1}^{5}(a_i^{\mathcal{U}})_{\mu\nu} = g^2 I_\mu(q)\left(\frac{i}{q^2}\right)I_\nu(-q). \tag{4.3}$$

Then, using Eq. (3.2), together with the fact that $I_\nu(-q) = -I_\nu(q)$, one obtains the following result

$$[\text{rhs}]_{\mu\nu} = \frac{q_\mu q_\nu}{q^2} g^2 I^2(q^2). \tag{4.4}$$

Therefore, equating Eq. (4.2) with Eq. (4.4) we find that the effective gluon mass is related to the transition amplitude through the simple formula (Minkowski space)

$$m^2(q^2) = g^2 I^2(q^2). \tag{4.5}$$

This last formula may be passed to Euclidean space, using the standard conversion rules, together with the expression for $I(q^2)$ given in Eq. (8.17). In particular, the transition to the

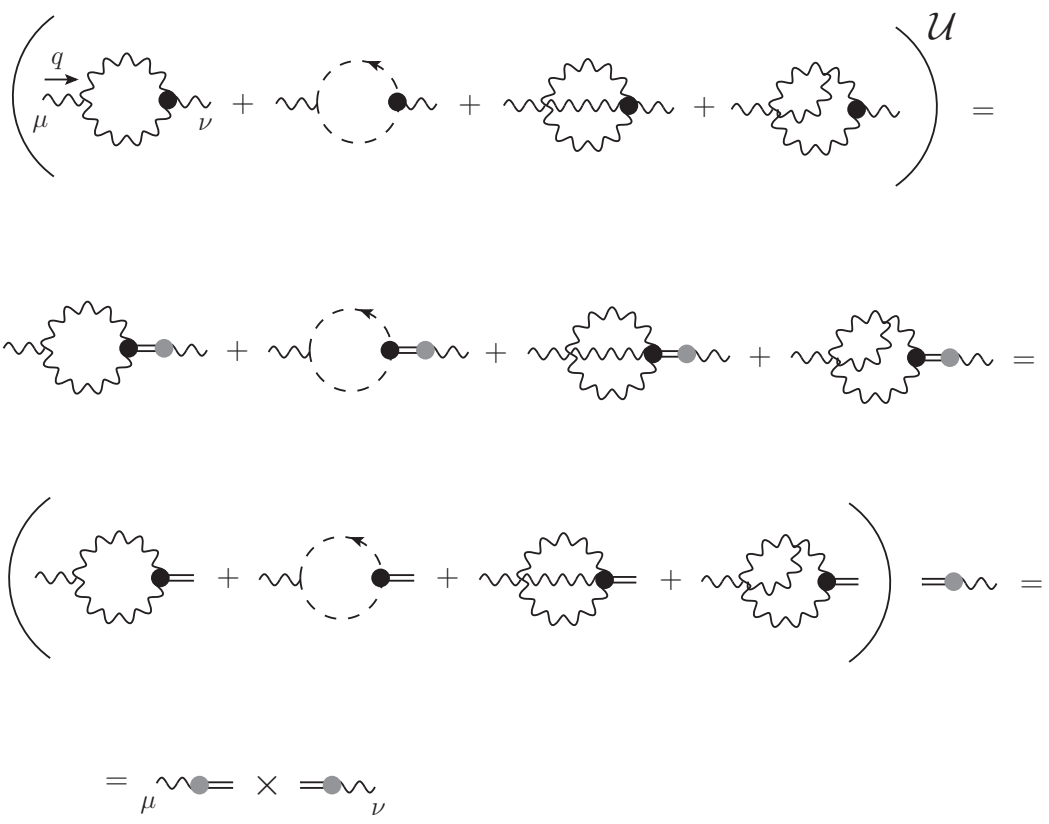

FIG. 8: General procedure for determining the contributions of the rhs of Eq. (4.1) to the effective gluon mass. Note that the vertices appearing in this figure correspond to the $\mathcal{U}$ parts of the full vertices Γ'.

Euclidean space proceeds by using the standard formulas that allow the conversion of the various Green's functions from the Minkowski momentum q^2 to the Euclidean $q_E^2 = -q^2 > 0$; specifically

$$\Delta_E(q_E^2) = -\Delta(-q_E^2); \quad m_E^2(q_E^2) = m^2(-q_E^2); \quad G_E(q_E^2) = G(-q_E^2); \quad \int_k = i\int_{k_E}. \tag{4.6}$$

As a consequence, we have $I_E(q_E^2) = -I(-q_E^2)$, so that

$$m_E^2(q_E^2) = g^2 I_E^2(q_E^2). \tag{4.7}$$

An immediate important implication of this last relation is that the gluon mass obtained is a positive-definite function for all values of the Euclidean momenta, as expected on physical grounds.

Let us finally mention that the transversality of the full gluon self-energy [see Eq. (2.11)] guarantees that if one were to consider the part of the mass equation proportional to $g_{\mu\nu}$,

one would eventually obtain exactly the same relation given in Eq. (4.5). Note, however, that the corresponding derivation is far more subtle and laborious, and hinges crucially on the judicious use of a special integral identity (for a detailed treatment of this issue, see [21]).

V. THE BQI OF THE TRANSITION AMPLITUDES: SDE DERIVATION

We will now repeat the construction of the last section using the SDEs of the PT-BFM formalism. Specifically, we will derive the relations analogous to Eq. (4.5), which, in conjunction with the BQIs connecting the conventional and PT-BFM gluon propagators, will furnish a nontrivial relation between the corresponding transition amplitudes.

A. General considerations

In the PT-BFM formalism the natural separation of the gluonic field into a "quantum" (Q) and a "background" (B) gives rise to an extended set of Feynman rules, and leads to an increase in the type of possible Green's functions that one may consider. In the case of the gluonic two-point function, in addition to the conventional QQ gluon propagator, Δ, two additional quantities appear: the QB propagator, $\widetilde{\Delta}$, mixing one quantum gluon with one background gluon, and the BB propagator, $\widehat{\Delta}$, with two background gluon legs. It turns out that these three propagators are related by the all-order identities (referred to as BQIs)

$$\Delta(q^2) = [1 + G(q^2)]\widetilde{\Delta}(q^2) = [1 + G(q^2)]^2\widehat{\Delta}(q^2). \tag{5.1}$$

The function $G(q^2)$, whose role in enforcing these crucial relations is instrumental, is defined as the $g_{\mu\nu}$ form factor of a special two-point function, given by (see Fig. 9)

$$\begin{aligned}\Lambda_{\mu\nu}(q) &= -ig^2 C_A \int_k \Delta^{\sigma}_{\mu}(k) D(q-k) H_{\nu\sigma}(-q, q-k, k) \\ &= g_{\mu\nu} G(q^2) + \frac{q_\mu q_\nu}{q^2} L(q^2),\end{aligned} \tag{5.2}$$

where C_A denotes the Casimir eigenvalue of the adjoint representation (N for $SU(N)$), $d = 4 - \epsilon$ is the space-time dimension, and we have introduced the integral measure

$$\int_k \equiv \frac{\mu^\epsilon}{(2\pi)^d} \int \mathrm{d}^d k, \tag{5.3}$$

with μ the 't Hooft mass. In addition, $D^{ab}(q^2) = \delta^{ab} D(q^2)$ is the ghost propagator, and $H_{\nu\sigma}$ is the gluon-ghost kernel [61, 62]. The dressed loop expansion of Λ and H is shown in Fig. 9.

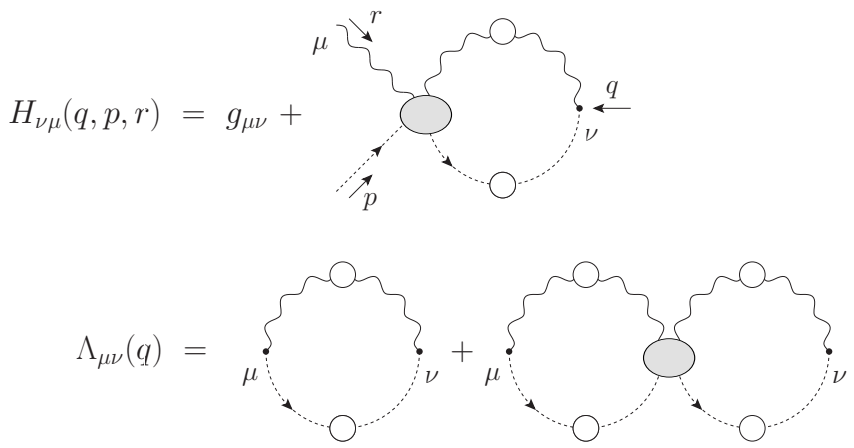

FIG. 9: Definitions and conventions of the auxiliary functions Λ and H.

Notice that the standard ghost-gluon vertex Γ_μ is obtained from $H_{\nu\mu}$ simply through the contraction

$$q^\nu H_{\nu\mu}(q,p,r) = -\Gamma_\mu(r,q,p). \tag{5.4}$$

Finally, in the Landau gauge only, the form factors $G(q^2)$ and $L(q^2)$ are linked to the ghost dressing function

$$F(q^2) = q^2 D(q^2) \tag{5.5}$$

by means of the all-order relation [57, 63–65]

$$F^{-1}(q^2) = 1 + G(q^2) + L(q^2)\,, \tag{5.6}$$

which will be extensively used in the ensuing analysis.

Returning to Eq. (5.1), it is important to recognize that the two basic functions constituting the gluon propagators, namely $J_m(q^2)$and $m^2(q^2)$, satisfy Eq. (5.1) individually [13]. In particular, the corresponding masses are related by

$$\widehat{m}^2(q^2) = [1 + G(q^2)]\widetilde{m}^2(q^2) = [1 + G(q^2)]^2 m^2(q^2). \tag{5.7}$$

Finally, in order to obtain from the SDEs of the PT-BFM propagators a mass formula analogous to that of Eq. (4.5), one needs to introduce the appropriate transition amplitude connecting the background gluon with the massless excitation. This new transition amplitude, whose diagrammatic representation is shown in Fig. 10, allows us to write the $\widetilde{\mathcal{U}}$ part of the corresponding pole vertices in the BFM as

$$\widetilde{\mathcal{U}}_{\alpha\{\ldots\}}(q,\ldots) = \widetilde{I}_\alpha(q)\frac{i}{q^2}B_{\{\ldots\}}(q,\ldots). \tag{5.8}$$

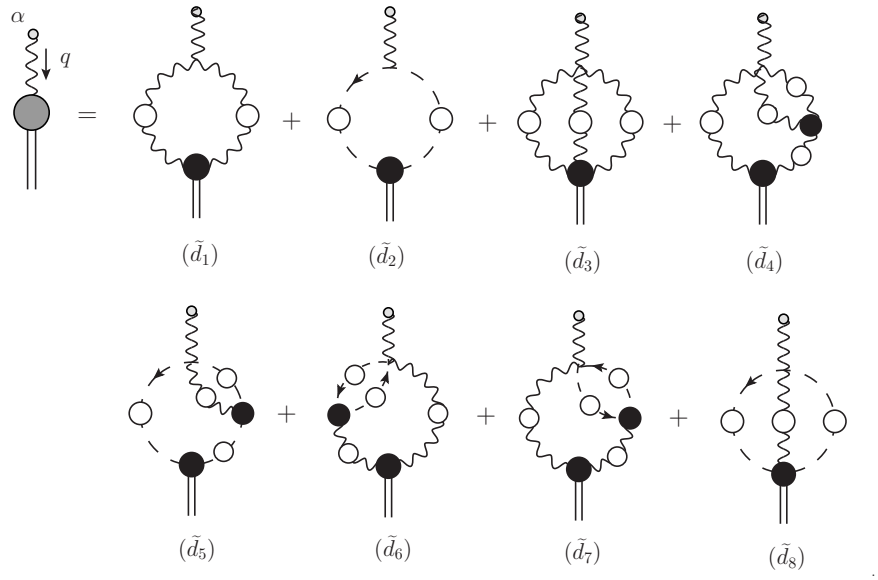

FIG. 10: Diagrammatic representation of the background transition amplitude $\widetilde{I}_\alpha(q)$.

Observe that only the transition amplitude is modified in this expression with respect to Eq. (3.4) when we go to the BFM. This is so because the only background field is the one carrying the momentum q, while all other fields are quantum (*i.e.*, they are common to the PT-BFM and conventional descriptions).

B. Relating the transition amplitudes through the SDEs of the PT-BFM

Consider the SDE for the QB propagator, connecting a quantum and a background field, given by the expression

$$\widetilde{\Delta}^{-1}(q^2)P_{\mu\nu}(q) = q^2 P_{\mu\nu}(q) + i\sum_{i=1}^{6}(a_i)_{\mu\nu}, \tag{5.9}$$

with the diagrams (a_i) shown in Fig. 11. Note that the diagrams are separated into three blocks, each of which is individually transverse; this special property of "block-wise" transversality is particular to the PT-BFM scheme.

Let us now apply the diagrammatic procedure shown in Fig. 8 to the new set of diagrams appearing in this SDE. Evidently, the quantity to be factored out from all diagrams comprising the $\widetilde{\mathcal{U}}$-related part of the SDE is $\widetilde{I}(q^2)$. Then, it is easy to recognize that the (sub) diagrams composing the other factor coincide precisely with those shown in the first line of

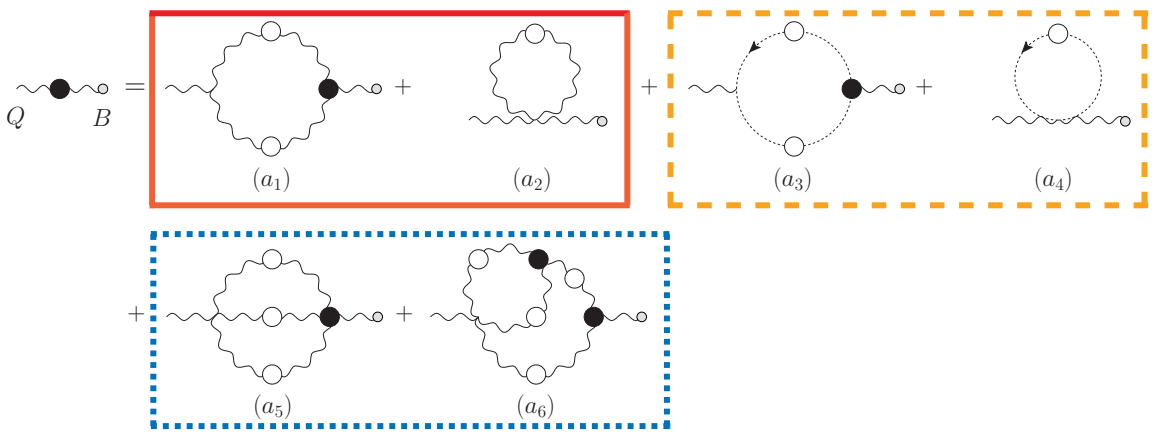

FIG. 11: SDE obeyed by the gluon self-energy with one quantum (Q) and one background gluon (B) entering. Each box encloses a set of diagrams forming a transverse subgroup. The small gray circles appearing on the external legs (entering from the right, only!) are used to indicate background gluons.

Fig. 5, thus giving rise to $I(q^2)$ again. Thus we arrive at the following expression for the mass of the QB propagator,

$$\widetilde{m}^2(q^2) = g^2 I(q^2)\widetilde{I}(q^2). \tag{5.10}$$

At this point one may use the BQI of Eq. (5.7) to replace $\widetilde{m}^2(q^2)$ in favor of $m^2(q^2)$ on the lhs of Eq. (5.10), namely

$$m^2(q^2) = \frac{g^2 I(q^2)\widetilde{I}(q^2)}{1+G(q^2)}. \tag{5.11}$$

Note that this last substitution is legitimate, because the corresponding SDEs have been considered in their full, untruncated version (all diagrams kept); therefore the masses obtained from them are the same exact quantities that satisfy the BQI.

Then, direct comparison with Eq. (4.5) furnishes the central relation

$$\widetilde{I}(q^2) = [1+G(q^2)]I(q^2). \tag{5.12}$$

Interestingly enough, this relation emerges as a self-consistency requirement between the results obtained from two formally different, but physically equivalent, versions of the gluon propagator SDE.

Furthermore, due to the special structure of Eq. (5.8), where only the transition amplitude knows if the q-leg is quantum or background, the result Eq. (5.12) implies that the part $\widetilde{\mathcal{U}}$

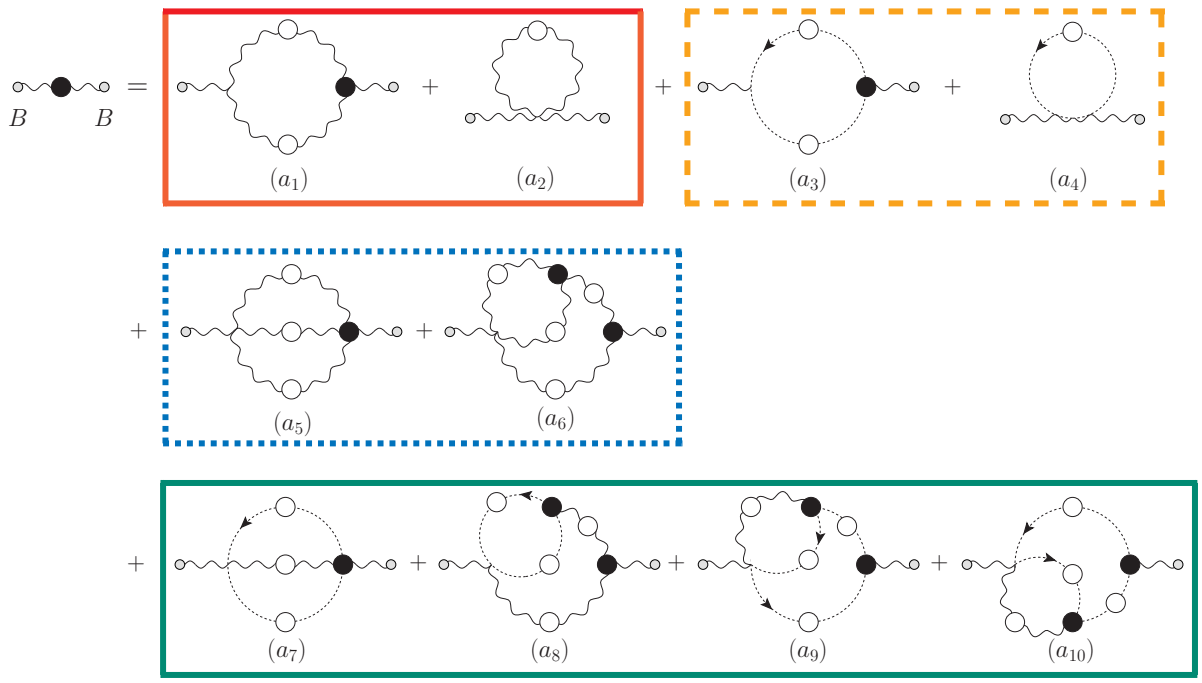

FIG. 12: SDE obeyed by the gluon self-energy with two background gluons (B) entering. The graphs inside each box form a transverse subgroup. External background legs are indicated by the small gray circles.

of the pole vertices must also satisfy the same BQI, namely (suppressing indices)

$$\widetilde{\mathcal{U}} = [1 + G(q^2)]\mathcal{U}. \tag{5.13}$$

Finally, let us consider for completeness the SDE for the BB propagator connecting two background gluons, given by the expression

$$\widehat{\Delta}^{-1}(q^2)P_{\mu\nu}(q) = q^2 P_{\mu\nu}(q) + i\sum_{i=1}^{10}(a_i)_{\mu\nu}, \tag{5.14}$$

where the diagrams (a_i) appearing on the rhs of the equation are shown in Fig. 12, arranged again into individually transverse blocks.

Repeating the procedure of Fig. 8 for this last SDE, we see that, as in the QB case, the common quantity to be factored out from all diagrams is again $\widetilde{I}(q^2)$. Then, the corresponding sum of (sub) diagrams coincides precisely with those of Fig. 10, thus giving rise to another $\widetilde{I}(q^2)$. As a result, one obtains

$$\widehat{m}^2(q^2) = g^2\widetilde{I}^2(q^2). \tag{5.15}$$

It should be easy to verify at this point that the direct use of Eq. (5.7) and subsequent comparison with Eq. (4.5) [or with Eq. (5.10)], furnishes again the result of Eq. (5.12).

VI. THREE-GLUON POLE VERTEX

In the previous section the basic relations Eq. (5.12) and Eq. (5.13) have been derived at the level of the SDEs, by appealing to the general properties of the massless bound state formalism and the BQIs relating the gluon propagators in the PT-BFM formalism. In the next two subsections we will derive the same relations from the pole parts of the Q^3 vertex and the BQ^2 vertex. Specifically, in the first subsection we derive in detail the closed form of these vertices, while in the next we identify their $\mathcal{U}$ parts, and carry out a direct comparison.

A. Explicit construction

As has been explained in detail in the early [16–20] and recent literature [21, 66], in order to preserve the gauge invariance of the theory in the presence of gauge boson masses, the usual vertices must be supplemented by pole parts. In particular, the pole part of the BQ^2 vertex must satisfy the following WI and STIs [21, 66],

$$\begin{aligned}
&q^{\alpha}\widetilde{V}_{\alpha\mu\nu}(q,r,p) = m^2(r^2)P_{\mu\nu}(r) - m^2(p^2)P_{\mu\nu}(p),\\
&r^{\mu}\widetilde{V}_{\alpha\mu\nu}(q,r,p) = F(r^2)[m^2(p^2)P^{\mu}_{\nu}(p)\widetilde{H}_{\mu\alpha}(p,r,q) - \widetilde{m}^2(q^2)P^{\mu}_{\alpha}(q)H_{\mu\nu}(q,r,p)],\\
&p^{\nu}\widetilde{V}_{\alpha\mu\nu}(q,r,p) = F(p^2)[\widetilde{m}^2(q^2)P^{\nu}_{\alpha}(q)H_{\nu\mu}(q,p,r) - m^2(r^2)P^{\nu}_{\mu}(r)\widetilde{H}_{\nu\alpha}(r,p,q)]. \qquad (6.1)
\end{aligned}$$

The quantity $\widetilde{H}$ is given by the same diagrammatic representation as that of H, shown in Fig. 9, but with the incoming gluon field replaced by a background one.

In the pole part of the Q^3 vertex, the leg associated with q_α is quantum instead of background, and, as a consequence, the Abelian-like WI [first in Eq. (6.1)] is replaced by an STI, namely

$$q^{\alpha}V_{\alpha\mu\nu}(q,r,p) = F(q^2)[m^2(r^2)P^{\alpha}_{\mu}(r)H_{\alpha\nu}(r,q,p) - m^2(p^2)P^{\alpha}_{\nu}(p)H_{\alpha\mu}(p,q,r)]. \qquad (6.2)$$

The STIs with respect to the other two legs are those of Eq. (6.1), but with the "tilded" quantities replaced by conventional ones.

It turns out that the explicit closed form of the two pole vertices in question, namely $\widetilde{V}$ and V, may be determined from the STIs they satisfy, and the requirement of complete longitudinality, *i.e.*, the condition Eq. (2.9). Specifically, opening up the transverse projectors in Eq. (2.9), one can write the entire vertex in terms of its own divergences,

$$\begin{aligned}\widetilde{V}_{\alpha\mu\nu}(q,r,p) &= \frac{q_\alpha}{q^2}q^\beta\widetilde{V}_{\beta\mu\nu} + \frac{r_\mu}{r^2}r^\rho\widetilde{V}_{\alpha\rho\nu} + \frac{p_\nu}{p^2}p^\sigma\widetilde{V}_{\alpha\mu\sigma} - \frac{q_\alpha r_\mu}{q^2r^2}q^\beta r^\rho\widetilde{V}_{\beta\rho\nu} - \frac{q_\alpha p_\nu}{q^2p^2}q^\beta p^\sigma\widetilde{V}_{\beta\mu\sigma} \\ &- \frac{r_\mu p_\nu}{r^2p^2}r^\rho p^\sigma\widetilde{V}_{\alpha\rho\sigma} + \frac{q_\alpha r_\mu p_\nu}{q^2r^2p^2}q^\beta r^\rho p^\sigma\widetilde{V}_{\beta\rho\sigma}. \end{aligned} \tag{6.3}$$

Note that the last term will not contribute because if we apply the STI's,

$$q^\beta r^\rho p^\sigma\widetilde{V}_{\beta\rho\sigma}(q,r,p) = 0. \tag{6.4}$$

So, using Eq. (6.1) to evaluate the various terms, and after a straightforward rearrangement, we obtain the following expression for the pole part of the BQ^2 vertex,

$$\begin{aligned}\widetilde{V}_{\alpha\mu\nu}(q,r,p) &= \frac{q_\alpha}{q^2}[m^2(r^2) - m^2(p^2)]P^\rho_\mu(r)P_{\rho\nu}(p) \\ &+ D(r^2)[m^2(p^2)P^\rho_\nu(p)\widetilde{H}_{\rho\alpha}(p,r,q) - \widetilde{m}^2(q^2)P^\rho_\alpha(q)P^\sigma_\nu(p)H_{\rho\sigma}(q,r,p)]r_\mu \\ &+ D(p^2)[\widetilde{m}^2(q^2)P^\rho_\alpha(q)H_{\rho\mu}(q,p,r) - m^2(r^2)P^\rho_\mu(r)\widetilde{H}_{\rho\alpha}(r,p,q)]p_\nu. \end{aligned} \tag{6.5}$$

Applying the same procedure, but using now the STIs of Eq. (6.2), together with the condition of Eq. (2.9), we derive the closed expression for the pole part of the Q^3 vertex,

$$\begin{aligned}V_{\alpha\mu\nu}(q,r,p) &= D(q^2)[m^2(r^2)H_{\rho\sigma}(r,q,p) - m^2(p^2)H_{\sigma\rho}(p,q,r)]P^\rho_\mu(r)P^\sigma_\nu(p)q_\alpha \\ &+ D(r^2)[m^2(p^2)P^\rho_\nu(p)H_{\rho\alpha}(p,r,q) - m^2(q^2)P^\rho_\alpha(q)P^\sigma_\nu(p)H_{\rho\sigma}(q,r,p)]r_\mu \\ &+ D(p^2)[m^2(q^2)P^\rho_\alpha(q)H_{\rho\mu}(q,p,r) - m^2(r^2)P^\rho_\mu(r)H_{\rho\alpha}(r,p,q)]p_\nu. \end{aligned} \tag{6.6}$$

Let us discuss next certain issues related to the self-consistency of the previous vertex construction. Notice that, in order to obtain the expressions in Eq. (6.5) and Eq. (6.6), one must apply sequentially the WI and the STIs. In doing so, the Bose symmetry of both vertices is no longer explicit, and the result obtained is not manifestly symmetric under the exchange of the quantum gluon legs. Furthermore, seemingly different expressions are obtained, depending on which of the two momenta acts first on $\widetilde{V}$ or V. However, if one imposes the simple requirement of algebraic commutativity between the WI and the STIs satisfied by the three-gluon vertex, the Bose symmetry becomes manifest. For example, using Eq. (6.5) we can see that the elementary requirement

$$q^\alpha r^\mu\widetilde{V}_{\alpha\mu\nu}(q,r,p) = r^\mu q^\alpha\widetilde{V}_{\alpha\mu\nu}(q,r,p), \tag{6.7}$$

gives raise to the following identity

$$F(r^2)P^{\mu}_{\nu}(p)q^{\alpha}\widetilde{H}_{\mu\alpha}(p,r,q) = -r_{\mu}P^{\mu}_{\nu}(p). \tag{6.8}$$

A similar identity is obtained by imposing the requirement of Eq. (6.7) at the level of V, namely

$$F(r^2)P^{\mu}_{\nu}(p)q^{\alpha}H_{\mu\alpha}(p,r,q) = -F(q^2)P^{\mu}_{\nu}(p)r^{\alpha}H_{\mu\alpha}(p,q,r). \tag{6.9}$$

Quite interestingly, the identities in Eq. (6.8) and Eq. (6.9) are a direct consequence of the WI and the STI that the kernels H and $\widetilde{H}$ satisfy, when they are contracted with the momentum of the background or quantum gluon leg, namely [67]

$$\begin{aligned} q^{\alpha}\widetilde{H}_{\mu\alpha}(p,r,q) &= -p_{\mu}F^{-1}(p^2) - r_{\mu}F^{-1}(r^2), \\ q^{\alpha}H_{\mu\alpha}(p,r,q) &= -F(q^2)[p_{\mu}F^{-1}(p^2)C(p,q,r) + r^{\alpha}F^{-1}(r^2)H_{\mu\alpha}(p,q,r)], \end{aligned} \tag{6.10}$$

where $C(p,q,r)$ is an auxiliary ghost function.

Indeed, use of Eq. (6.10) into Eq. (6.8) and Eq. (6.9), respectively, leads to a trivial identity. Conversely, one may actually derive Eq. (6.10) from Eq. (6.8) and Eq. (6.9); for example, starting with Eq. (6.8), and using also the identities [67]

$$\begin{aligned} p^{\mu}\widetilde{H}_{\mu\alpha}(p,r,q) &= r_{\alpha}F^{-1}(r^2) - \widetilde{\Gamma}_{\alpha}(q,p,r), \\ q^{\alpha}\widetilde{\Gamma}_{\alpha}(q,p,r) &= p^2F^{-1}(p^2) - r^2F^{-1}(r^2), \end{aligned} \tag{6.11}$$

one can easily reproduce Eq. (6.10).

Evidently, these constraints allow us to cast the pole part of the BQ^2 vertex into a manifestly Bose symmetric form with respect to the quantum legs,

$$\widetilde{V}_{\alpha\mu\nu}(q,r,p) = \frac{q_{\alpha}}{q^2}[m^2(r^2) - m^2(p^2)]P^{\rho}_{\mu}(r)P_{\rho\nu}(p) + \widetilde{S}_{\alpha\mu\nu}(q,r,p) - \widetilde{S}_{\alpha\nu\mu}(q,p,r), \tag{6.12}$$

with

$$\begin{aligned} \widetilde{S}_{\alpha\mu\nu}(q,r,p) &= D(r^2)m^2(p^2)P^{\rho}_{\nu}(p)\widetilde{H}_{\rho\alpha}(p,r,q)r_{\mu} \\ &- \frac{r_{\mu}}{2}D(r^2)\widetilde{m}^2(q^2)P^{\rho}_{\alpha}(q)[g^{\sigma}_{\nu} + P^{\sigma}_{\nu}(p)]H_{\rho\sigma}(q,r,p). \end{aligned} \tag{6.13}$$

Finally, for the pole part of the Q^3 vertex, the Bose symmetric expression reads

$$V_{\alpha\mu\nu}(q,r,p) = S_{\alpha\mu\nu}(q,r,p) - S_{\mu\alpha\nu}(r,q,p) - S_{\nu\mu\alpha}(p,r,q), \tag{6.14}$$

with

$$S_{\alpha\mu\nu}(q,r,p) = \frac{q_\alpha}{2}D(q^2)m^2(r^2)P^\rho_\mu(r)[g^\sigma_\nu + P^\sigma_\nu(p)]H_{\rho\sigma}(r,q,p) - \frac{q_\alpha}{2}D(q^2)m^2(p^2)P^\rho_\nu(p)[g^\sigma_\mu + P^\sigma_\mu(r)]H_{\rho\sigma}(p,q,r). \quad (6.15)$$

Note the fact that, as it should be, setting in Eqs.(6.12)-(6.14) the tree-level values $F = 1$ and $H_{\mu\nu} = g_{\mu\nu}$ for the ghost dressing function and the gluon-ghost kernel, respectively, one recovers the expression for the "abelianized" three-gluon vertex first presented in [68].

B. Transition BQI derived from the pole vertices

We next identify from the explicit expressions for the BQ^2 and Q^3 pole vertices the terms $\widetilde{\mathcal{U}}$ and $\mathcal{U}$. To that end, and in complete accordance with the discussion presented in subsection II B, we apply a kinematic and a dynamical criterion, namely (i) determine U by collecting all terms containing the tensorial structure q_α/q^2, and (ii) extract $\mathcal{U}$ by discarding (and reassigning them to $\mathcal{U}'$) all terms that, when inserted into the SDE of the gluon self-energy, do not survive the $q \to 0$ limit, *i.e.*, do not contribute to the gluon mass equation. The final objective is to infer the validity of the BQI of Eq. (5.13), connecting $\widetilde{\mathcal{U}}$ and $\mathcal{U}$.

Applying criterion (i), and denoting by $\widetilde{U}$ and U the resulting expressions, it is straightforward to obtain from Eq. (6.12)

$$\widetilde{U}_{\alpha\mu\nu}(q,r,p) = \frac{q_\alpha}{q^2}\left\{m^2(r^2)P^\rho_\mu(r)P_{\rho\nu}(p) - \frac{r_\mu}{2}D(r^2)\widetilde{m}^2(q^2)[g^\rho_\nu + P^\rho_\nu(p)]\Gamma_\rho(p,q,r)\right\} - \binom{r\leftrightarrow p}{\mu\leftrightarrow\nu}, \quad (6.16)$$

where Eq. (5.4) has been applied in order to relate the contractions of the auxiliary ghost functions H with the conventional gluon-ghost vertices Γ_ρ, and $\binom{r\leftrightarrow p}{\mu\leftrightarrow\nu}$ is obtained from the term that is shown explicitly after carrying out the exchanges indicated. In addition, for the $\widetilde{R}$ part of the vertex we find

$$\widetilde{R}_{\alpha\mu\nu}(q,r,p) = \frac{r_\mu}{r^2}F(r^2)\left\{m^2(p^2)P^\rho_\nu(p)\widetilde{H}_{\rho\alpha}(p,r,q) - \frac{1}{2}\widetilde{m}^2(q^2)[g^\rho_\nu + P^\rho_\nu(p)]H_{\alpha\rho}(q,r,p)\right\} - \binom{r\leftrightarrow p}{\mu\leftrightarrow\nu}. \quad (6.17)$$

Similarly, from Eq. (6.14), and using the special STI Eq. (6.10), we obtain

$$\begin{aligned} U_{\alpha\mu\nu}(q,r,p) &= \frac{q_\alpha}{q^2}\Big\{F(q^2)m^2(r^2)H_{\rho\sigma}(r,q,p)P^\rho_\mu(r)P^\sigma_\nu(p) \\ &- \frac{r_\mu}{2}D(r^2)m^2(q^2)[g^\rho_\nu + P^\rho_\nu(p)]\Gamma_\rho(p,q,r)\Big\} - \binom{r\leftrightarrow p}{\mu\leftrightarrow\nu}, \end{aligned} \tag{6.18}$$

and

$$\begin{aligned} R_{\alpha\mu\nu}(q,r,p) &= \frac{r_\mu}{r^2}F(r^2)\Big\{m^2(p^2)P^\rho_\nu(p)H_{\rho\alpha}(p,r,q) - \frac{1}{2}m^2(q^2)[g^\rho_\nu + P^\rho_\nu(p)]H_{\alpha\rho}(q,r,p)\Big\} \\ &- \binom{r\leftrightarrow p}{\mu\leftrightarrow\nu}. \end{aligned} \tag{6.19}$$

Let us now assume for a moment that $\widetilde{U}=\widetilde{\mathcal{U}}$ and $U=\mathcal{U}$, as well as $\widetilde{R}=\widetilde{\mathcal{R}}$ and $R=\mathcal{R}$. Let us further use Eq. (5.7), and substitute $m^2(q^2)=\widetilde{m}^2(q^2)[1+G(q^2)]^{-1}$ into Eq. (6.18). Then, employing Eq. (5.6) valid in the Landau gauge, dropping $L(q^2)$ since $L(0)=0$ [thus applying effectively criterion (ii)], it is relatively easy to establish that the (would-be) $\widetilde{\mathcal{U}}$ and $\mathcal{U}$ fail to satisfy Eq. (5.13) due to the presence of a very particular term. Specifically, if $H_{\rho\sigma}\to g_{\rho\sigma}$ in the first line of Eq. (6.18), then the BQI of Eq. (5.13) would be satisfied.

Therefore, write the $H_{\rho\sigma}(r,q,p)$ in Eq. (6.18) as

$$H_{\rho\sigma}(r,q,p) = g_{\rho\sigma} + H^Q_{\rho\sigma}(r,q,p), \tag{6.20}$$

where the $g_{\rho\sigma}$ corresponds to the tree-level value of $H_{\rho\sigma}$, and $H^Q_{\rho\sigma}$ contains the all-order quantum corrections; an exactly analogous expression holds for $H_{\sigma\rho}(p,q,r)$, with $p\leftrightarrow r$. Note that in both cases the momentum q is carried by the ghost leg, see Fig. 13. Then, if we define the part $\mathcal{U}$ as [see Eq. (2.19)]

$$\mathcal{U}_{\alpha\mu\nu}(q,r,p) = U_{\alpha\mu\nu}(q,r,p) - \mathcal{U}'_{\alpha\mu\nu}(q,r,p), \tag{6.21}$$

with

$$\mathcal{U}'_{\alpha\mu\nu}(q,r,p) = \frac{q_\alpha}{q^2}F(q^2)m^2(r^2)P^\rho_\mu(r)P^\sigma_\nu(p)H^Q_{\rho\sigma}(r,q,p) - \binom{r\leftrightarrow p}{\mu\leftrightarrow\nu}, \tag{6.22}$$

it is clear that

$$\widetilde{\mathcal{U}}_{\alpha\mu\nu}(q,r,p) = [1+G(q^2)]\mathcal{U}_{\alpha\mu\nu}(q,r,p). \tag{6.23}$$

The real justification for discarding $\mathcal{U}'_{\alpha\mu\nu}$ from $U_{\alpha\mu\nu}$ is provided precisely by invoking criterion (*ii*): the discarded term does not survive the limit $q\to 0$ when inserted into the corresponding gluon SDE.

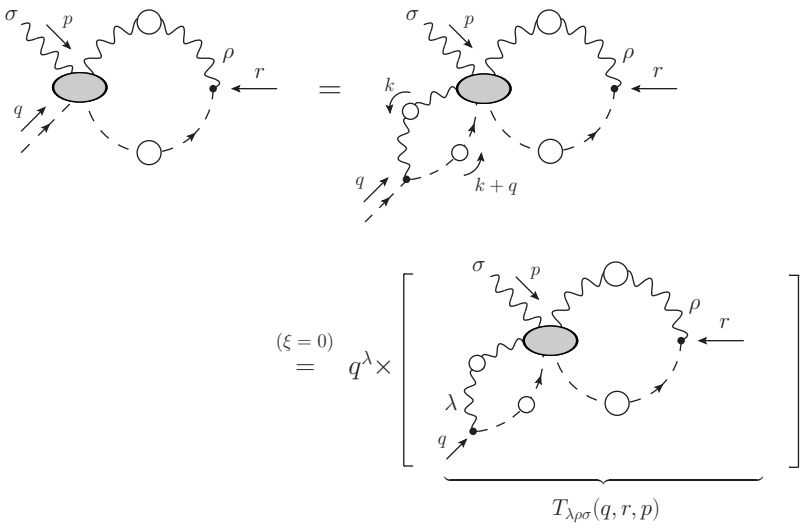

FIG. 13: Diagrammatic representation of Eq. (6.24).

To demonstrate that this is indeed so, note that in the Landau gauge $(k+q)^\lambda \Delta_{\lambda\sigma}(k) = q^\lambda \Delta_{\lambda\sigma}(k)$, and the momentum of the incoming ghost leg factorizes out of the loop integrals. This observation allows us to cast H^Q in the form

$$H^Q_{\rho\sigma}(r,q,p) = q^\lambda T_{\lambda\rho\sigma}(q,r,p). \tag{6.24}$$

where T simply represents the rest of the diagram (see Fig. 13). If we assume now that T has a finite (non-divergent) value in the limit $q \to 0$, then

$$\lim_{q\to 0} H^Q_{\rho\sigma}(r,q,p) = \lim_{q\to 0} q^\lambda T_{\lambda\rho\sigma}(q,r,p) = 0. \tag{6.25}$$

So, using Eq. (6.24), the term given in Eq. (6.22) becomes

$$\mathcal{U}'_{\alpha\mu\nu}(q,r,p) = \frac{q_\alpha q^\lambda}{q^2} F(q^2) m^2(r^2) P^\rho_\mu(r) P^\sigma_\nu(p) T_{\lambda\rho\sigma}(q,r,p) - \binom{r \leftrightarrow p}{\mu \leftrightarrow \nu}. \tag{6.26}$$

When $\mathcal{U}'_{\alpha\mu\nu}$ is written in this form, it is clear that its pole $1/q^2$ is actually compensated by $q_\alpha q^\lambda$, while the remaining terms cancel themselves when $r = -p$. Therefore, the entire term $\mathcal{U}'_{\alpha\mu\nu}$ vanishes as $q \to 0$, and should not be included in the $\mathcal{U}$ part of the Q^3 pole vertex.

Finally, returning to the identification $\widetilde{U} = \widetilde{\mathcal{U}}$, note that the expression in Eq. (6.16) does not get modified by the application of criterion (*ii*), because the above argument of discarding H^Q does not apply in this case. The reason for that is simply the channeling of the momenta in $H_{\rho\sigma}(q,r,p)$ and $H_{\rho\sigma}(q,p,r)$ (encoded into the gluon-ghost vertices Γ_ρ)

is different from that of $H_{\rho\sigma}(r,q,p)$; the momentum entering in the ghost leg is no longer q, but rather r or p, and the corresponding H^{Q}s do not satisfy Eq. (6.25). As a result, no terms need be discarded from $\widetilde{U}$, and, therefore, $\widetilde{\mathcal{U}}' = 0$.

Let us now cast $\mathcal{U}_{\alpha\mu\nu}(q,r,p)$ and $\widetilde{\mathcal{U}}_{\alpha\mu\nu}(q,r,p)$ into their canonical form of Eq. (3.4) and Eq. (5.8), respectively, namely

$$\begin{aligned}\mathcal{U}_{\alpha\mu\nu}(q,r,p) &= -\frac{q_\alpha}{q^2} I(q^2) B_{\mu\nu}(q,r,p), \\ \widetilde{\mathcal{U}}_{\alpha\mu\nu}(q,r,p) &= -\frac{q_\alpha}{q^2} \widetilde{I}(q^2) B_{\mu\nu}(q,r,p);\end{aligned} \tag{6.27}$$

the minus sign comes from the extra imaginary factor appearing in the Feynman rule of the effective vertex, see Fig. 5. The important point to recognize is that $B_{\mu\nu}(q,r,p)$ is common to both vertices, because the legs carrying r and p are quantum ones, and the difference induced due to the quantum or background nature of the leg carrying momentum q is entirely encoded into the form of the corresponding transition amplitudes, $I(q^2)$ and $\widetilde{I}(q^2)$, respectively. Then, Eq. (6.27) and Eq. (6.23) imply directly the validity of Eq. (5.12).

VII. DIAGRAMMATIC DEMONSTRATION OF THE BQI

It is well-known that the BQIs relating the conventional and BFM Green's functions are formally obtained by resorting to the powerful BV formalism. On the other hand, the PT (or its generalized version [31]) furnishes an equivalent diagrammatic derivation, which makes extensive use of the STIs satisfied by the kernels appearing in the SDEs of the Green's functions in question. In the previous sections the BQI of Eq. (5.12) relating the transition amplitudes $I(q^2)$ and $\widetilde{I}(q^2)$ has been obtained as a self-consistency requirement between two SDEs, and from the corresponding BQI relating $\mathcal{U}$ and $\widetilde{\mathcal{U}}$ (sections V and VI, respectively). The objective of this section is to carry out a PT-guided demonstration of this particular BQI, through the systematic conversion of the set of Feynman diagrams defining one transition amplitude into the set defining the other (shown in Figs. 5 and 10). Essentially this conversion proceeds by allowing the longitudinal (pinching) momenta contained in the tree-level three-gluon vertex [graph $(\widetilde{d}_1)$] to act on the adjacent kernel; therefore, as we will see, a crucial ingredient for completing this construction is the knowledge of the STI satisfied by the effective vertex $B_{\mu\nu}$. In addition, the requirement that the BQI be diagrammatically exact imposes a strong constraint on the set of ghost diagrams that

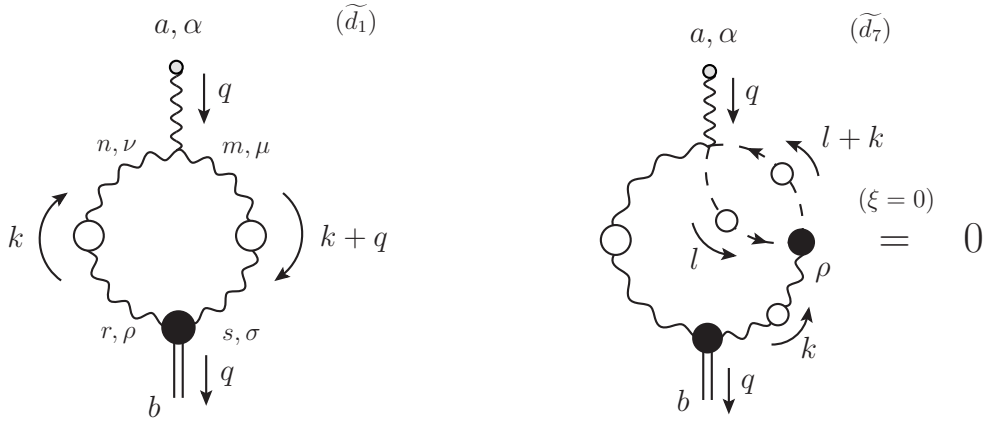

FIG. 14: Detailed representation of diagrams $(\widetilde{d_1})$ and $(\widetilde{d_7})$. Diagram $(\widetilde{d_1})$ has a symmetry factor 1/2; diagrams $(\widetilde{d_6})$ and $(\widetilde{d_7})$ vanish in the Landau gauge.

contribute to the transition amplitude, which may be translated (under mild assumptions) into the vanishing of the corresponding subset of B vertices.

A. The PT construction at the level of the transition amplitude

Let us start by considering the diagram $(\widetilde{d_1})$ of the background transition amplitude, shown in Fig. 14, whose contribution is given by

$$(\widetilde{d_1})_\alpha = \frac{i}{2} C_A \int_k \widetilde{\Gamma}^{(0)}_{\alpha\mu\nu} \Delta^{\mu\sigma}(k+q) \Delta^{\nu\rho}(k) B_{\rho\sigma}. \tag{7.1}$$

In order to avoid notational clutter we will suppress the arguments of the momenta in the vertices, which can be easily recovered from the figures. In what follows, the coupling and color dependence of the diagrams comprising the evaluation of $\widetilde{I}_\alpha(q)$ is restored by setting $(\widetilde{d_i})^{ab}_\alpha = g\delta^{ab}(\widetilde{d_i})_\alpha$.

We know that the tree-level vertex $\widetilde{\Gamma}^{(0)}_{\alpha\mu\nu}$ contains terms which are proportional to ξ^{-1}, so that one cannot take directly the limit $\xi = 0$ to work in the Landau gauge. Specifically, the tree-level part of the BQ^2 vertex is given by

$$\widetilde{\Gamma}^{(0)}_{\alpha\mu\nu}(q, -k-q, k) = \Gamma^{(0)}_{\alpha\mu\nu}(q, -k-q, k) - \frac{1}{\xi}\Gamma^{P}_{\alpha\mu\nu}(q, -k-q, k), \tag{7.2}$$

where the purely longitudinal "pinch part" Γ^P reads

$$\Gamma^{P}_{\alpha\mu\nu}(q, -k-q, k) = g_{\alpha\mu} k_\nu + g_{\alpha\nu}(k+q)_\mu, \tag{7.3}$$

and

$$\Gamma^{(0)}_{\alpha\mu\nu}(q,-k-q,k) = -(2k+q)_\alpha g_{\mu\nu} + (k-q)_\mu g_{\alpha\nu} + (2q+k)_\nu g_{\alpha\mu} \tag{7.4}$$

is the tree-level value of the conventional three-gluon vertex. Using then the decomposition Eq. (7.2), we obtain from Eq. (7.1)

$$(\widetilde{d}_1)_\alpha = (d_1)_\alpha - \frac{i}{2\xi} C_A \int_k \Gamma^P_{\alpha\mu\nu} \Delta^{\mu\sigma}(k+q) \Delta^{\nu\rho}(k) B_{\rho\sigma}. \tag{7.5}$$

Now, after the shifts $k+q \mapsto k$ and $k \mapsto -k$, and applying the antisymmetry property of the effective vertex, namely $B_{\rho\sigma} = -B_{\sigma\rho}$, the two contributions coming from the pinch part of the vertex in Eq. (7.5) sum up and cancel the symmetry factor, giving the result

$$(\widetilde{d}_1)_\alpha = (d_1)_\alpha - \frac{i}{\xi} C_A \int_k k_\nu \Delta^{\nu\rho}(k) \Delta^\sigma_\alpha(k+q) B_{\rho\sigma}. \tag{7.6}$$

Therefore, employing the identity

$$\frac{1}{\xi} k_\nu \Delta^{\nu\rho}(k) = \frac{k^\rho}{k^2}, \tag{7.7}$$

the ξ^{-1} term cancels, and we can project Eq. (7.6) to the Landau gauge ($\xi = 0$),

$$(\widetilde{d}_1)_\alpha = (d_1)_\alpha - i C_A \int_k \frac{k^\rho}{k^2} \Delta^\sigma_\alpha(k+q) B_{\rho\sigma}, \tag{7.8}$$

where the gluon propagator assumes a totally transverse form, *i.e.*, $\Delta_{\mu\nu}(k) = \Delta(k^2) P_{\mu\nu}(k)$.

At this point, in order to evaluate the integral on the rhs of Eq. (7.8), the knowledge of the STI satisfied by the effective vertex $B_{\rho\sigma}$ is required. Observe then that, if we compare Eq. (6.16) with Eq. (6.27), the following structure can be identified as the $B_{\mu\nu}$,

$$\begin{aligned} \widetilde{I}(q^2) B_{\mu\nu}(q,r,p) \;&=\; -m^2(r^2) P^\rho_\mu(r) P_{\rho\nu}(p) + \frac{r_\mu}{2} D(r^2) \widetilde{m}^2(q^2) [g^\rho_\nu + P^\rho_\nu(p)] \Gamma_\rho(p,q,r) \\ &-\; \binom{r \leftrightarrow p}{\mu \leftrightarrow \nu}. \end{aligned} \tag{7.9}$$

Therefore, contracting Eq. (7.9) with respect to the momentum r^μ, and breaking the transverse projector $P^\rho_\nu(p)$, we find

$$\begin{aligned} \widetilde{I}(q^2) r^\mu B_{\mu\nu}(q,r,p) \;&=\; F(r^2) \widetilde{m}^2(q^2) \Gamma_\nu(p,q,r) \\ &-\; \frac{p_\nu}{2p^2} \widetilde{m}^2(q^2) [F(r^2) p^\rho \Gamma_\rho(p,q,r) + F(p^2) r^\rho \Gamma_\rho(r,q,p)]. \end{aligned} \tag{7.10}$$

Now, the second term on the rhs does not contribute, since $p_\nu \to (k+q)_\sigma$ is annihilated by the transverse projector of $\Delta^\sigma_\alpha(k+q)$ in Eq. (7.8).

Thus, employing the STI Eq. (7.10), adapted to our kinematical configuration, *i.e.*, $r=-k$ and $p=k+q$, together with Eq. (5.10), Eq. (7.8) becomes

$$\begin{aligned}(\widetilde{d}_1)_\alpha &= (d_1)_\alpha + ig^2 C_A I(q^2)\int_k \Delta^\sigma_\alpha(k+q)D(k)\Gamma_\sigma \\ &= (d_1)_\alpha - ig^2 C_A I(q^2) q^\lambda \int_k \Delta^\sigma_\alpha(k+q)D(k)H_{\lambda\sigma}, \end{aligned} \tag{7.11}$$

where, in the second line, Eq. (5.4) has been used.

At this point, one recognizes on the rhs of Eq. (7.11) the appearance of the auxiliary two-point function Λ, defined in Eq. (5.2); so, we obtain

$$\begin{aligned}(\widetilde{d}_1)_\alpha &= (d_1)_\alpha + I(q^2) q^\lambda \Lambda_{\alpha\lambda}(q) \\ &= (d_1)_\alpha + [G(q^2)+L(q^2)] I_\alpha(q). \end{aligned} \tag{7.12}$$

Finally, since $L(0)=0$, one can drop the term $L(q^2)$, exactly as was done in the previous section (and with the same justification), finally arriving at

$$(\widetilde{d}_1)_\alpha = (d_1)_\alpha + G(q^2) I_\alpha(q). \tag{7.13}$$

Let us next observe that *(i)* diagrams (d_3) and (d_4) in Fig. 5 can be converted automatically to background ones, given that the tree-level vertex BQ^3 is identical to the conventional four gluon vertex Q^4, and that *(ii)* diagrams $(\widetilde{d}_6)$ and $(\widetilde{d}_7)$ vanish in the Landau gauge, see Fig. 14; this happens because, after integration, the contribution of the ghost loop nested inside them will be proportional to k^ρ, and it will vanish when contracted with the $\Delta_{\rho\rho'}(k)$. So,

$$(\widetilde{d}_3) = (d_3)\,, \quad (\widetilde{d}_4) = (d_4)\,, \quad (\widetilde{d}_6) = (\widetilde{d}_7) = 0\,. \tag{7.14}$$

Therefore, comparing Eq. (7.13) and Eq. (7.14) with Eq. (5.12), we see that, in order for the full BQI to be diagrammatically realized, the relation

$$(d_2) = (\widetilde{d}_2) + (\widetilde{d}_5) + (\widetilde{d}_8) \tag{7.15}$$

should be satisfied.

B. A constraint on the ghost sector

In the previous subsection we have derived Eq. (7.15) from the requirement that the basic BQI Eq. (5.12) be diagrammatically realized. The common characteristic of all diagrams

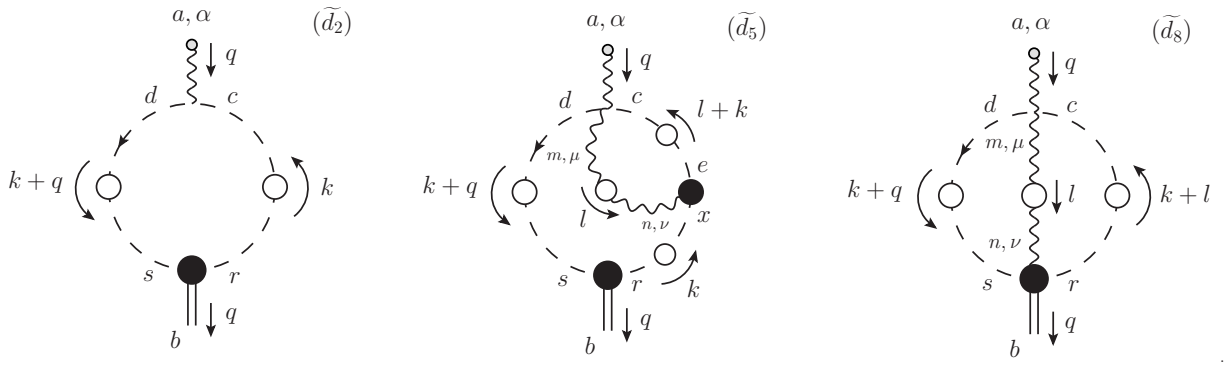

FIG. 15: Detailed representation of the diagrams $(\widetilde{d}_2)$, $(\widetilde{d}_5)$, and $(\widetilde{d}_8)$, appearing in Eq. (7.15).

comprising Eq. (7.15) is that they contain vertices B which mix the nonperturbative massless bound-state with two ghosts. Given that the nature of these vertices is practically unknown, it would be interesting to inquire what restriction Eq. (7.15) may impose on their structure, and whether this restriction is compatible with other pieces of nonperturbative information on the ghost sector of Yang-Mills theories.

In the formulas that follow, color factors are shown explicitly, while the arguments of the momenta in the vertices are suppressed as before. Then, the diagrams appearing in Eq. (7.15) are given by

$$\begin{aligned}
(d_2)^{ab}_{\alpha} &= -igC_A\delta^{ab}\int_k \Gamma^{(0)}_{\alpha} D(k)D(k+q)B\,,\\
(\widetilde{d}_2)^{ab}_{\alpha} &= -igC_A\delta^{ab}\int_k \widetilde{\Gamma}^{(0)}_{\alpha} D(k)D(k+q)B\,,\\
(\widetilde{d}_5)^{ab}_{\alpha} &= g^3C_A^2\delta^{ab}\int_k \widetilde{\Gamma}^{(0)}_{\alpha\mu} D(k)D(k+q)B\int_l D(k+l)\Delta^{\mu\nu}(l)\Gamma_{\nu}\,,\\
(\widetilde{d}_8)^{ab}_{\alpha} &= g^2 f^{adx}f^{xcm}\int_k\int_l D(k+q)D(k+l)\Delta^{\nu}_{\alpha}(l)B^{bcmd}_{\nu}\,.
\end{aligned} \tag{7.16}$$

Observe that the pole part of the internal gluon-ghost vertex Γ_ν does not contribute to $(\widetilde{d}_5)$ in the Landau gauge, due to the longitudinality condition that it ought to satisfy. Therefore, only the regular part of this vertex survives in $(\widetilde{d}_5)$.

We will next use the SDE satisfied by the ghost propagator $D(k)$, written as [35]

$$g^2C_AD(k)\int_l D(k+l)\Delta^{\mu\nu}(l)\Gamma_\nu = ik_\alpha[D(k)-D^{(0)}(k)], \tag{7.17}$$

to cast $(\widetilde{d}_5)$ in the form

$$(\widetilde{d}_5)^{ab}_{\alpha} = igC_A\delta^{ab}\int_k k_\alpha[D(k)-D^{(0)}(k)]D(k+q)B. \tag{7.18}$$

Substituting the above results into Eq. (7.15), we arrive at the integral constraint

$$iC_A\delta^{ab}\int_k \frac{k_\alpha}{k^2}D(k+q)B = gf^{adx}f^{xcm}\int_k\int_l D(k+q)D(k+l)\Delta^\nu_\alpha(l)B^{bcmd}_\nu\,, \tag{7.19}$$

relating B and B_ν.

We next turn to the full BFM gluon-ghost vertex, $\widetilde{\Gamma}$, which satisfies the following all-order WI [33, 35]

$$q^\alpha\widetilde{\Gamma}_\alpha(q,r,p) = D^{-1}(r^2) - D^{-1}(p^2). \tag{7.20}$$

Let us suppose that, due to nonperturbative dynamics, $\widetilde{\Gamma}$ acquires a pole part; then, in full analogy to Eq. (2.8), we define

$$\widetilde{\Gamma}'_\alpha(q,r,p) = \widetilde{\Gamma}_\alpha(q,r,p) + \widetilde{V}_\alpha(q,r,p), \tag{7.21}$$

as the sum of a regular part and a pole part. In addition, and again in analogy with Eq. (2.12), we will assume that also the ghost propagator acquires a mass term, to be denoted by $m_c^2(q^2)$, and so

$$D^{-1}(q^2) = q^2F^{-1}(q^2) \longmapsto D_m^{-1}(q^2) = q^2F_m^{-1}(q^2) - m_c^2(q^2). \tag{7.22}$$

Then, it is clear that we must have

$$\begin{aligned} q^\alpha\widetilde{\Gamma}_\alpha(q,r,p) &= r^2F_m^{-1}(r^2) - p^2F_m^{-1}(p^2)\,, \\ q^\alpha\widetilde{V}_\alpha(q,r,p) &= m_c^2(p^2) - m_c^2(r^2)\,, \end{aligned} \tag{7.23}$$

so that finally

$$q^\alpha\widetilde{\Gamma}'_\alpha(q,r,p) = D_m^{-1}(r^2) - D_m^{-1}(p^2)\,, \tag{7.24}$$

as it should.

If we now assume the existence of a massless pole in the q-channel which, in addition, satisfies the longitudinality condition

$$P^\beta_\alpha(q)\widetilde{V}_\beta(q,r,p) = 0, \tag{7.25}$$

then, the WI obeyed by $\widetilde{V}_\alpha(q,r,p)$, may be solved, yielding

$$\widetilde{V}_\alpha(q,r,p) = \frac{q_\alpha}{q^2}[m_c^2(p^2) - m_c^2(r^2)]. \tag{7.26}$$

Note that $\widetilde{V}_\alpha(q,r,p)$ is purely of the $\widetilde{\mathcal{U}}$ type (no $\widetilde{\mathcal{R}}$ terms).

Then, using the corresponding expression Eq. (5.8) for this vertex

$$\widetilde{V}_\alpha(q,r,p) = -\frac{q_\alpha}{q^2}\widetilde{I}(q^2)B(q,r,p), \tag{7.27}$$

and equating with Eq. (7.26), we obtain a relation between the effective vertex B and the mass-like term in the ghost propagator

$$\widetilde{I}(q^2)B(q,r,p) = m_c^2(r^2) - m_c^2(p^2). \tag{7.28}$$

Now, large-volume lattice results [4–7, 9], together with a variety of analytic studies [42, 43, 45], establish that *(i)* the ghost propagator in the Landau gauge remains massless, which means that $m_c^2(q^2) = 0$. *(ii)* The dressing function $F_m(q^2)$ is infrared-finite; this happens essentially due to the fact that the gluon mass $m^2(q^2)$ regulates it, in the same way as J_m, namely through the qualitative replacement $\ln q^2 \to \ln(q^2 + m^2)$ [see discussion after Eq. (2.12)]. Therefore, since $m_c^2(q^2) = 0$ but $\widetilde{I}(q^2) \neq 0$, Eq. (7.28) implies that $B = 0$.

Returning to the constraint of Eq. (7.19) and setting $B = 0$, we have that the integral on the rhs involving B_ν must vanish also. Even though from this statement one cannot mathematically conclude that B_ν must vanish identically, this seems to be the most reasonable scenario. Indeed, the rather fine-tuned alternative would invoke a subtle conspiracy between the various form factors comprising B_ν, which ought to combine in such a way (and change signs correspondingly) as to make this integral vanish.

VIII. COMPARISON OF THE TWO MASS-GENERATING FORMALISMS

In this section we first derive the full expression for the transition amplitude in the Landau gauge, and then we show that, when judiciously combined with Eq. (4.5) and Eq. (8.19), it gives rise to an integral equation for the gluon mass, which *coincides exactly* with the one obtained within the SDE formalism of [21]. We then proceed to a brief study of how the distinct approximations employed within the two formalism lead to differences in the form of the gluon masses obtained.

A. Exact formal equivalence

From the analysis presented in the previous section we have concluded that diagrams with ghost loops do not contribute to the transition amplitude. Furthermore, one may

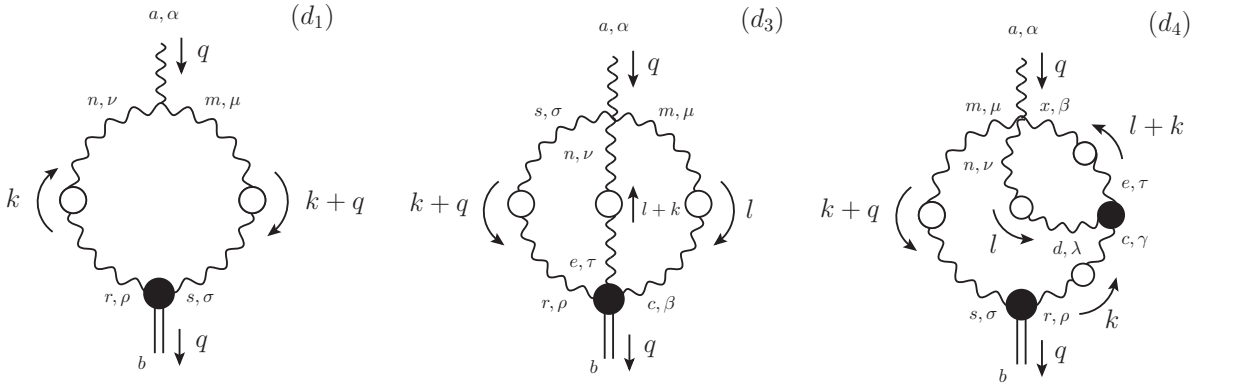

FIG. 16: Configuration for the diagrams of $I_\alpha(q)$ that contain only gluon loops. The symmetry factors for the diagrams are $S(d_1, d_3, d_4) = (1/2, 1/6, 1/2)$.

demonstrate that diagram (d_3) in Fig. 16, which contains the effective vertex $B_{\rho\tau\beta}$ mixing three quantum gluons with the bound state, vanishes in the Landau gauge. Effectively, with the configuration shown in Fig. 16, we can write down the contribution of this diagram,

$$(d_3)^{ab}_{\alpha} = \frac{1}{6}\int_k\int_l \Gamma^{(0)amns}_{\alpha\mu\nu\sigma}\Delta^{\sigma\rho}_{sr}(k+q)\Delta^{\nu\tau}_{ne}(l+k)\Delta^{\mu\beta}_{mc}(l)B^{brec}_{\rho\tau\beta}. \tag{8.1}$$

As in the preceding sections, the arguments of the momenta in the vertices have been suppressed. Observe that, in order to evaluate this diagram in the Landau gauge, one should know how three transverse projectors act over the effective vertex $B_{\rho\tau\beta}$. Consider then the decomposition Eq. (2.21) for the BQ^3 pole vertex,

$$\widetilde{V}_{\lambda\rho\tau\beta}(q,r,p,l) = \widetilde{\mathcal{U}}_{\lambda\rho\tau\beta}(q,r,p,l) + \widetilde{\mathcal{R}}_{\lambda\rho\tau\beta}(q,r,p,l), \tag{8.2}$$

where, according with the discussion carry out in Section II, the $\widetilde{\mathcal{R}}$ part of the vertex satisfies the transversality condition

$$P^{\sigma\rho}(r)P^{\nu\tau}(p)P^{\mu\beta}(l)\widetilde{\mathcal{R}}_{\lambda\rho\tau\beta}(q,r,p,l) = 0. \tag{8.3}$$

Thus, when Eq. (2.9) is applied for the case of the BQ^3 pole vertex, namely, four transverse projectors canceling the vertex, we obtain from Eq. (8.2) the following result

$$P^{\sigma\rho}(r)P^{\nu\tau}(p)P^{\mu\beta}(l)\widetilde{\mathcal{U}}_{\alpha\rho\tau\beta}(q,r,p,l) = \frac{q_\alpha}{q^2}P^{\sigma\rho}(r)P^{\nu\tau}(p)P^{\mu\beta}(l)q^\lambda\widetilde{V}_{\lambda\rho\tau\beta}(q,r,p,l). \tag{8.4}$$

On the other hand Eq. (5.8) becomes for the $\widetilde{\mathcal{U}}$ part of this pole vertex,

$$\widetilde{\mathcal{U}}_{\alpha\rho\tau\beta}(q,r,p,l) = ig\frac{q_\alpha}{q^2}\widetilde{I}(q^2)B_{\rho\tau\beta}(q,r,p,l). \tag{8.5}$$

Therefore, applying three transverse projectors on Eq. (8.5) and equating the result with Eq. (8.4) we can relate the effective vertex $B_{\rho\tau\beta}$ with the WI satisfied by the BQ^3 pole vertex when it is contracted with respect to the momentum of the background gluon leg, *i.e.*,

$$ig\widetilde{I}(q^2)P^{\sigma\rho}(r)P^{\nu\tau}(p)P^{\mu\beta}(l)B_{\rho\tau\beta}(q,r,p,l) = P^{\sigma\rho}(r)P^{\nu\tau}(p)P^{\mu\beta}(l)q^{\lambda}\widetilde{V}_{\lambda\rho\tau\beta}(q,r,p,l). \tag{8.6}$$

Once the above connection has been established through Eq. (8.6), one may repeat the steps presented in subsection VI B of [21], thus demonstrating the vanishing of diagram (d_3).

Therefore, the full transition amplitude will be given in the Landau gauge solely by the sum of diagrams (d_1) and (d_4). Thus, applying the conventions of Fig. 16, we obtain for diagram (d_1) the expression,

$$(d_1)_{\alpha} = \frac{i}{2}C_A\int_k \Gamma^{(0)}_{\alpha\mu\nu}\Delta^{\mu\sigma}(k+q)\Delta^{\nu\rho}(k)B_{\rho\sigma}. \tag{8.7}$$

One observes that the above integral has one free Lorentz index, which only can be saturated by the external momentum q. So, using the elementary WI for the tree-level three-gluon vertex,

$$q^{\lambda}\Gamma^{(0)}_{\lambda\mu\nu}(q,-k-q,k) = k^2P_{\mu\nu}(k) - (k+q)^2P_{\mu\nu}(k+q), \tag{8.8}$$

and after the appropriate shifts in the integrated momentum, we deduce in the Landau gauge the result,

$$(d_1)_{\alpha} = \frac{q_{\alpha}}{q^2}q^{\lambda}(d_1)_{\lambda} = iC_A\frac{q_{\alpha}}{q^2}\int_k k^2\Delta^{\rho}_{\mu}(k)\Delta^{\mu\sigma}(k+q)B_{\rho\sigma}. \tag{8.9}$$

Now, diagram (d_4) contains the tree-level four-gluon vertex $\Gamma^{(0)}_{\alpha\mu\nu\beta}$. After the color algebra and using the standard Feynman rule for this vertex, we obtain for the prefactor of the diagram,

$$\frac{i}{2}gf^{bcm}f^{cxn}\Gamma^{(0)amnx}_{\alpha\mu\nu\beta} = \frac{3}{4}g^3C_A^2(g_{\alpha\nu}g_{\mu\beta} - g_{\alpha\beta}g_{\mu\nu})\delta^{ab}. \tag{8.10}$$

Thus, we get in the Landau gauge the following expression,

$$(d_4)_{\alpha} = \frac{3}{4}g^2C_A^2(g_{\alpha\nu}g_{\mu\beta} - g_{\alpha\beta}g_{\mu\nu})\int_k \Delta^{\mu\sigma}(k+q)\Delta^{\rho\gamma}(k)Y^{\nu\beta}_{\gamma}(k)B_{\rho\sigma}, \tag{8.11}$$

where we have defined the loop integral

$$Y^{\nu\beta}_{\gamma}(k) = \int_l \Delta^{\nu\lambda}(l)\Delta^{\beta\tau}(k+l)\Gamma_{\gamma\tau\lambda}. \tag{8.12}$$

Note that in the Landau gauge, the fully-dressed three-gluon vertex appearing in this integral only contains the regular part, since the transverse projectors of the gluon propagators trigger Eq. (2.9) for that vertex.

As before, the integral in Eq. (8.11) only can be saturated by the external momentum q. Moreover, due to the Bose symmetry of the three-gluon vertex is straightforward to show that the integral Eq. (8.12) is antisymmetric under the $\nu \leftrightarrow \beta$ exchange, and given also the antisymmetry of the prefactor under the same exchange, one can write

$$Y_\gamma^{\nu\beta}(k) = (k^\nu g_\gamma^\beta - k^\beta g_\gamma^\nu) Y(k^2) \quad ; \quad Y(k^2) = \frac{1}{d-1}\frac{k_\nu}{k^2} g_\beta^\gamma Y_\gamma^{\nu\beta}(k). \tag{8.13}$$

With these observations, Eq. (8.11) can be cast in the form

$$(d_4)_\alpha = \frac{q_\alpha}{q^2} q^\lambda (d_4)_\lambda = \frac{3}{2} g^2 C_A^2 \frac{q_\alpha}{q^2} \int_k [(kq) g_{\mu\gamma} + q_\mu q_\gamma] Y(k^2) \Delta^{\mu\sigma}(k+q) \Delta^{\rho\gamma}(k) B_{\rho\sigma}. \tag{8.14}$$

Employing now the results obtained for diagrams (d_1) and (d_4), we derive the complete expression of the transition amplitude in the Landau gauge [see Eq. (3.3)],

$$\begin{aligned} I(q^2) \;&=\; \frac{q^\alpha}{q^2}[(d_1) + (d_4)]_\alpha = \frac{i}{q^2} C_A \int_k k^2 \Delta_\mu^\rho(k) \Delta^{\mu\sigma}(k+q) B_{\rho\sigma} \\ &+\; \frac{3}{2}\frac{g^2 C_A^2}{q^2} \int_k [(kq) g_{\mu\gamma} + q_\mu q_\gamma] Y(k^2) \Delta^{\mu\sigma}(k+q) \Delta^{\rho\gamma}(k) B_{\rho\sigma}. \end{aligned} \tag{8.15}$$

To proceed further, we decompose the effective vertex $B_{\rho\sigma}$ in the tensor basis

$$B_{\rho\sigma} = B_1 g_{\rho\sigma} + B_2 q_\rho q_\sigma + B_3 (k+q)_\rho (k+q)_\sigma + B_4 k_\rho q_\sigma + B_5 k_\rho (k+q)_\sigma. \tag{8.16}$$

When this decomposition is inserted in Eq. (8.15), only the form factor B_1 survives, since in [26] was shown that $B_2 = 0$ and the rest of form factors are canceled in the Landau gauge by the transverse projectors. Therefore, Eq. (8.15) becomes

$$\begin{aligned} I(q^2) \;&=\; \frac{i}{q^2} C_A \int_k k^2 \Delta_\mu^\rho(k) \Delta_\rho^\mu(k+q) B_1 \\ &+\; \frac{3}{2}\frac{g^2 C_A^2}{q^2} \int_k [(kq) g_{\mu\gamma} + q_\mu q_\gamma] Y(k^2) \Delta_\rho^\mu(k+q) \Delta^{\rho\gamma}(k) B_1, \end{aligned} \tag{8.17}$$

which, quite remarkably, allows to express the full transition amplitude, for general value of q^2, in terms of one single form factor, namely, B_1. At this point we arrive at the crucial observation which enables us to relate the mass equation obtained in the context of the PT-BFM formalism with the bound-state formalism showing that, indeed both formalisms

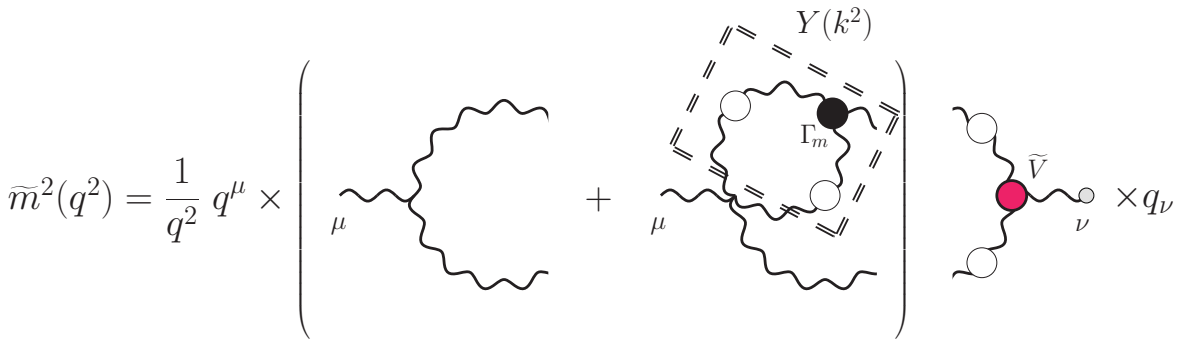

FIG. 17: Concise diagrammatic representation of the combined operations leading to the all-order gluon mass equation; $\widetilde{m}^2(q^2)$ is defined in Eq. (5.7).

are self-consistent and interconnected. From Eq. (7.9) one may obtain, after identify the $g_{\mu\nu}$ component, a closed expression for the form factor B_1 in terms of the gluon mass

$$\begin{aligned}\widetilde{I}(q^2)B_1(q,r,p) &= [1+G(q^2)]I(q^2)B_1(q,r,p)\\ &= m^2(p^2)-m^2(r^2),\end{aligned} \tag{8.18}$$

where the BQI Eq. (5.12) has been applied. Therefore, using this relation and after a straightforward rearrangement Eq. (8.17) yields

$$I^2(q^2) = \frac{iC_A}{1+G(q^2)}\frac{1}{q^2}\int_k \Delta_{\gamma\rho}(k)\Delta^\rho_\mu(k+q)\mathcal{K}^{\gamma\mu}_{SD}(q,k)m^2(k^2). \tag{8.19}$$

In this expression, the quantity

$$\begin{aligned}\mathcal{K}^{\gamma\mu}_{SD}(q,k) &= g^{\gamma\mu}[(k+q)^2-k^2]\left\{1+\frac{3}{4}ig^2C_A[Y(k+q)+Y(k)]\right\}\\ &+ \frac{3}{4}ig^2C_A(q^2g^{\gamma\mu}-2q^\gamma q^\mu)[Y(k+q)-Y(k)].\end{aligned} \tag{8.20}$$

represents the SD kernel obtained from the sum of the two graphs on the rhs of the equation depicted in Fig. 17. Thus, using the mass formula Eq. (4.5) on the lhs of Eq. (8.19), we arrive to the result

$$m^2(q^2) = \frac{ig^2C_A}{1+G(q^2)}\frac{1}{q^2}\int_k m^2(k^2)\Delta_{\gamma\rho}(k)\Delta^\rho_\mu(k+q)\mathcal{K}^{\gamma\mu}_{SD}(q,k)\,. \tag{8.21}$$

Quite remarkably, this result coincides *exactly* with the full mass equation derived in [21] from the SDE of the gluon propagator, following the procedure shown pictorially in Fig. 17, whose formal aspects are considerably different compared to those of the massless bound-state formalism. The emergence of an identical dynamical equation for the gluon mass provides an impressive self-consistency check between these two formalisms.

B. Differences in the numerical implementation

At this point it is important to recognize that, although formally equivalent, the two approaches ["SDE" vs "massless bound-state"] entail vastly different procedures for obtaining the desired quantity, namely the functional form of $m^2(q^2)$. Given that in practice approximations must be carried out to the fundamental equations of both formalisms, the results obtained for $m^2(q^2)$ will be in general different; indeed, the formal coincidence proved above is only valid when all equations involved are treated exactly.

To appreciate this issue in some quantitative detail, recall that, within the massless bound-state formalism, the starting point for obtaining the momentum-dependence of the gluon mass is Eq. (8.18). Specifically, in the limit $q \to 0$ one obtains the following exact relation for the derivative of the effective gluon mass (Euclidean space) [26]

$$\frac{dm^2(p^2)}{dp^2} = -\widetilde{I}(0) B_1'(p^2), \tag{8.22}$$

where the prime denotes differentiation with respect to $(p+q)^2$ and subsequently taking the limit $q \to 0$, *i.e.*,

$$B_1'(p^2) \equiv \lim_{q\to 0} \left\{ \frac{\partial B_1(q, -p-q, p)}{\partial\,(p+q)^2} \right\} . \tag{8.23}$$

It turns out that the function $B_1'(p^2)$ satisfies its own homogeneous BSE [see Section III, Fig. 6 and discussion below], of the general form

$$B_1'(p^2) = \int_k \mathcal{K}(p,k) B_1'(k^2), \tag{8.24}$$

where $\mathcal{K}$ corresponds to the Bethe-Salpeter four-gluon kernel, shown in line A of Fig. 18 [see also Fig. 6]. Evidently, the exact treatment of this equation would require the complete knowledge of the four-gluon kernel, which, however, is a largely unexplored quantity. Therefore, in order to obtain an approximate solution to Eq. (8.24), one resorts to the "improved" ladder approximation of this kernel, shown diagrammatically in Fig. 18, by dressing the gluon propagators but keeping the vertices at tree-level. Then, the numerical solution of Eq. (8.24) yields for $B_1'(q^2)$ the function shown on the left panel of Fig. 19.

With this information at hand, the gluon mass may be obtained through direct integration of Eq. (8.22), namely

$$m^2(q^2) = m^2(0) - \widetilde{I}(0) \int_0^{q^2} dx B_1'(x). \tag{8.25}$$

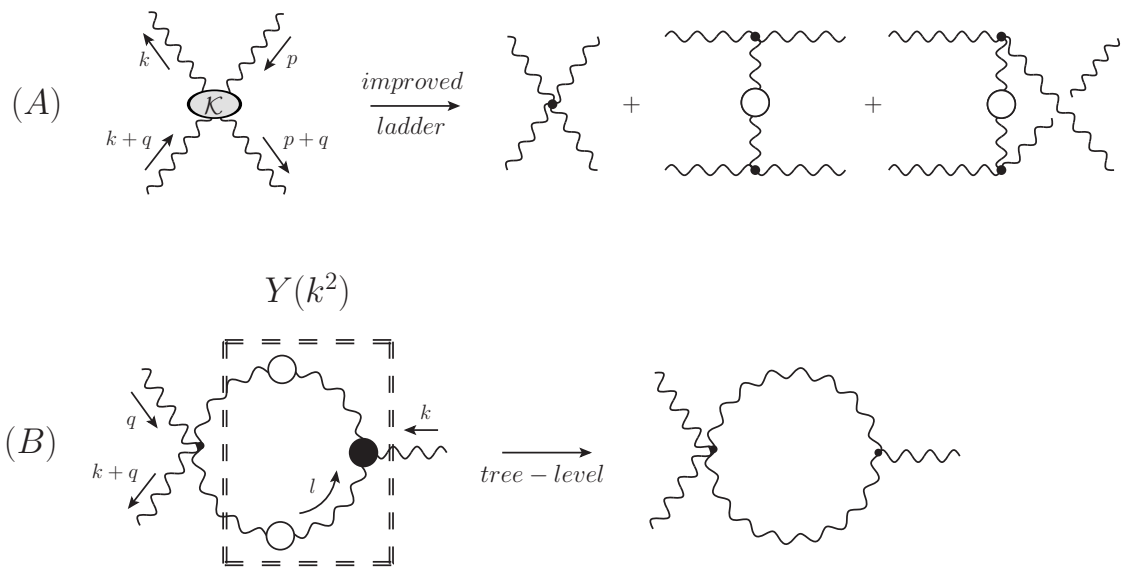

FIG. 18: (A) The kernel $\mathcal{K}$ of the BSE satisfied by B_1' and the approximation introduced in [26]. (B) The full kernel $\mathcal{K}_{SD}$ of the mass equation, and the approximation employed in [21].

As for the constant $\widetilde{I}(0)$, using the BQI Eq. (5.12), as well as Eq. (5.6) and Eq. (4.5), one obtains

$$\widetilde{I}(0) = F^{-1}(0)I(0) = F^{-1}(0)\sqrt{\frac{m^2(0)}{g^2}} = F^{-1}(0)\sqrt{\frac{\Delta^{-1}(0)}{4\pi\alpha_s}}, \tag{8.26}$$

which allow us to estimate $\widetilde{I}(0)$ from the lattice values of the ghost dressing function and the gluon propagator at zero momentum, treating α_s as an adjustable parameter. Thus, one finally arrives at the dynamical gluon mass shown on the right panel of Fig. 19 [red (continuous) curve] [26].

Let us now turn to the SDE approach [21], and compare with the corresponding approximations and numerical results. In this case the basic dynamical equation is that of Eq. (8.21), whose central ingredient is the quantity $Y(k^2)$, entering into the kernel $\mathcal{K}_{SD}$, given in Eq. (8.20). The quantity $Y(k^2)$, shown in line B of Fig. 18, involves the *fully-dressed* three-gluon vertex, which too is rather poorly known. As a result, in [21] the quantity $Y(k^2)$ has been approximated by its perturbative (one-loop) expression, by replacing the fully dressed internal gluon propagators and three-gluon vertex by their tree-level values, as shown in Fig. 18. Under these approximations, the numerical treatment of Eq. (8.21) gives rise to the solution shown on the right panel of Fig. 19 [blue (dotted) curve].

Note that both masses have been normalized in such a way as to coincide at the origin;

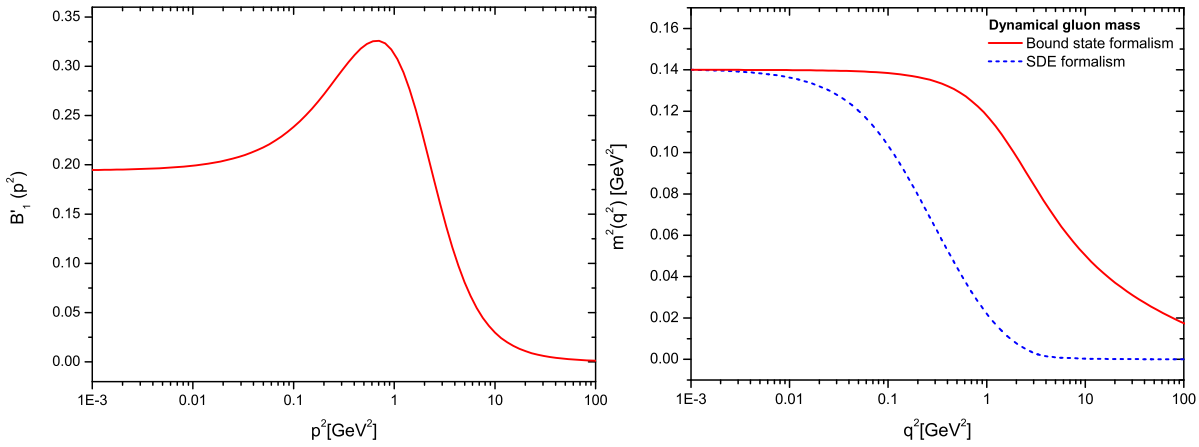

FIG. 19: (Left panel): The general form of $B_1'(q^2)$ obtained from the numerical solution of Eq. (8.24), in the improved ladder approximation. (Right panel): The two solutions obtained for the gluon mass within the massless bound-state [red (solid)] and SDE [blue (dotted)] approaches

in particular, $m^2(0) = 0.14$ GeV^2, which is the saturation point reached by the gluon propagator simulated on the lattice, when renormalized at $\mu = 4.3$ GeV (the last point available in the ultraviolet tail). It is clear from this direct comparison that the two formally equivalent approaches lead to qualitatively similar results, which, however, do not coincide, due to the inequivalence of the approximations employed.

IX. CONCLUSIONS

In this article we have studied in detail the mechanism of gluon mass generation within the massless bound-state formalism, which constitutes the formal framework for the systematic implementation of the Schwinger mechanism at the level of four-dimensional non-Abelian gauge theories. The main ingredient of this formalism is the dynamical formation of massless bound-states, which give rise to effective vertices containing massless poles; these latter vertices trigger the Schwinger mechanism, and allow for the gauge-invariant generation of an effective gluon mass. The principal advantage of this approach is its ability to relate the gluon mass directly to quantities that are usually employed in the physics of bound-states, such as transition amplitudes and bound-state wave functions, as well as obtaining the dynamical evolution through a BSE instead of a SDE [see, for example, Eq. (4.5), Eq. (8.25) and Eq. (8.24)].

A central result of the present work is the formal equivalence between the massless bound-state formalism and the corresponding approach based on the direct study of the SDE of the gluon propagator [21]. In particular, the powerful relations provided by the STIs of the theory, such as Eq. (8.18), allowed us to demonstrate the exact coincidence of the integral equations governing the momentum evolution of the gluon mass in both formalisms.

Note that this formal equivalence, in addition to serving as a clear indication of an underlying consistency, opens up the possibility of extracting useful, albeit indirect, information on the structure of certain quantities appearing in one formalism, from results obtained within the other. It seems, for instance, that a nonperturbative approximation for the quantity Y (see the SDE of Eq. (8.21)) is easier to obtain than a corresponding approximation for the four-gluon kernel $\mathcal{K}$, a central ingredient of the BSE in Eq. (8.24). Indeed, Y involves the fully dressed three-gluon vertex, which may be partially reconstructed, by means of a gauge-technique Ansatz, from the STIs that it satisfies [56]; to be sure, lattice simulation may also be valuable in this effort [69]. Instead, nonperturbative approximations for $\mathcal{K}$ are much more difficult to obtain with the present technology. Therefore, one might be able to use a finer solution for $m^2(q^2)$, obtained from the SDE of Eq. (8.21) by going beyond the one-loop approximation for Y, to infer the behavior of the kernel $\mathcal{K}$, at least for some special kinematic configurations. This information, in turn, may be helpful in a variety of unrelated studies that involve this particular kernel.

Even though the derivation of various of the results presented here relies on the use of the Landau gauge, it would seem that the general features of the massless bound-state formalism remain valid for any value of the gauge-fixing parameter, within the general class of linear covariant gauges. It would be therefore most interesting to derive the corresponding dynamical equations for different gauges, and explore whether the gluon mass generation mechanism persists away from the Landau gauge. In fact, such studies may be complemented by parallel lattice simulations of the corresponding gluon and ghost propagators [70, 71].

In a similar vein, lattice simulations carried out in the BFM [72, 73] may prove instrumental for verifying explicitly some of the formal relations employed throughout this work. For example, the BQI of Eq. (5.1) may be directly probed, for a wide range of momenta, if $\widehat{\Delta}(q^2)$ is simulated in the background Landau gauge; for a prediction, see [64]. In fact, even the knowledge of just the corresponding saturation point, $\widehat{\Delta}(0)$, would enable one to check the validity of Eq. (5.7) at $q^2 = 0$.

Acknowledgments

This research is supported by the Spanish MEYC under grant FPA2011-23596. We thank A.C. Aguilar and D. Binosi for several useful discussions.

---

[1] J. M. Cornwall, Phys. Rev. D **26**, 1453 (1982).

[2] C. W. Bernard, Nucl. Phys. B **219**, 341 (1983).

[3] J. F. Donoghue, Phys. Rev. D **29**, 2559 (1984).

[4] A. Cucchieri and T. Mendes, PoS **LAT2007**, 297 (2007).

[5] A. Cucchieri and T. Mendes, Phys. Rev. Lett. **100**, 241601 (2008).

[6] A. Cucchieri and T. Mendes, Phys. Rev. D **81**, 016005 (2010).

[7] I. L. Bogolubsky, E. M. Ilgenfritz, M. Muller-Preussker and A. Sternbeck, PoS LATTICE, 290 (2007).

[8] P. O. Bowman *et al.*, Phys. Rev. D **76**, 094505 (2007).

[9] I. L. Bogolubsky, E. M. Ilgenfritz, M. Muller-Preussker and A. Sternbeck, Phys. Lett. B **676**, 69 (2009).

[10] O. Oliveira and P. J. Silva, PoS **LAT2009**, 226 (2009).

[11] T. Iritani, H. Suganuma and H. Iida, Phys. Rev. D **80**, 114505 (2009).

[12] A. C. Aguilar, D. Binosi and J. Papavassiliou, Phys. Rev. D **78**, 025010 (2008).

[13] A. C. Aguilar, D. Binosi and J. Papavassiliou, Phys. Rev. D **84**, 085026 (2011).

[14] J. S. Schwinger, Phys. Rev. **125**, 397 (1962).

[15] J. S. Schwinger, Phys. Rev. **128**, 2425 (1962).

[16] R. Jackiw and K. Johnson, Phys. Rev. D **8**, 2386 (1973).

[17] R. Jackiw, In *Erice 1973, Proceedings, Laws Of Hadronic Matter*, New York 1975, 225-251 and M I T Cambridge - COO-3069-190 (73,REC.AUG 74) 23p.

[18] J. M. Cornwall and R. E. Norton, Phys. Rev. D **8** 3338 (1973).

[19] E. Eichten and F. Feinberg, Phys. Rev. D **10**, 3254 (1974).

[20] E. C. Poggio, E. Tomboulis and S. H. Tye, Phys. Rev. D **11**, 2839 (1975).

[21] D. Binosi, D. Ibanez and J. Papavassiliou, Phys. Rev. D **86**, 085033 (2012).

[22] A. P. Szczepaniak and E. S. Swanson, Phys. Rev. D **65**, 025012 (2002).

[23] A. P. Szczepaniak, Phys. Rev. D **69**, 074031 (2004).

[24] D. Epple, H. Reinhardt, W. Schleifenbaum and A. P. Szczepaniak, Phys. Rev. D **77**, 085007 (2008).

[25] A. P. Szczepaniak and H. H. Matevosyan, Phys. Rev. D **81**, 094007 (2010).

[26] A. C. Aguilar, D. Ibanez, V. Mathieu and J. Papavassiliou, Phys. Rev. D **85**, 014018 (2012)

[27] J. M. Cornwall and J. Papavassiliou, Phys. Rev. D **40**, 3474 (1989).

[28] D. Binosi and J. Papavassiliou, Phys. Rev. D **66**(R), 111901 (2002).

[29] D. Binosi and J. Papavassiliou, J. Phys. G **30**, 203 (2004).

[30] D. Binosi and J. Papavassiliou, Phys. Rept. **479**, 1 (2009).

[31] A. Pilaftsis, Nucl. Phys. B **487**, 467 (1997).

[32] See, e.g., L. F. Abbott, Nucl. Phys. B **185**, 189 (1981), and references therein.

[33] A. C. Aguilar and J. Papavassiliou, JHEP **0612**, 012 (2006).

[34] D. Binosi and J. Papavassiliou, Phys. Rev. D **77**(R), 061702 (2008).

[35] D. Binosi and J. Papavassiliou, JHEP **0811**, 063 (2008).

[36] P. A. Grassi, T. Hurth and M. Steinhauser, Annals Phys. **288**, 197 (2001).

[37] D. Binosi and J. Papavassiliou, Phys. Rev. D **66**, 025024 (2002).

[38] I. A. Batalin, G. A. Vilkovisky, Phys. Lett. **B69**, 309-312 (1977).

[39] I. A. Batalin, G. A. Vilkovisky, Phys. Lett. **B102**, 27-31 (1981).

[40] A. C. Aguilar, A. A. Natale and P. S. Rodrigues da Silva, Phys. Rev. Lett. **90**, 152001 (2003).

[41] A. C. Aguilar and A. A. Natale, JHEP **0408**, 057 (2004).

[42] D. Dudal, J. A. Gracey, S. P. Sorella, N. Vandersickel and H. Verschelde, Phys. Rev. D **78** (2008) 065047.

[43] P. Boucaud, J. P. Leroy, A. Le Yaouanc, J. Micheli, O. Pene and J. Rodriguez-Quintero, JHEP **0806** (2008) 099.

[44] C. S. Fischer, A. Maas and J. M. Pawlowski, Annals Phys. **324**, 2408 (2009).

[45] J. Rodriguez-Quintero, PoS LC **2010** (2010) 023.

[46] P. Bicudo and O. Oliveira, PoS LATTICE **2010**, 269 (2010).

[47] O. Oliveira and P. Bicudo, J. Phys. G G **38**, 045003 (2011).

[48] K. -I. Kondo, Phys. Rev. D **84**, 061702 (2011).

[49] S. -x. Qin, L. Chang, Y. -x. Liu, C. D. Roberts and D. J. Wilson, Phys. Rev. C **84**, 042202 (2011).

[50] P. Gonzalez, V. Mathieu and V. Vento, Phys. Rev. D **84**, 114008 (2011).

[51] M. R. Pennington and D. J. Wilson, Phys. Rev. D **84**, 119901 (2011).

[52] A. Bashir, R. Bermudez, L. Chang and C. D. Roberts, Phys. Rev. C **85**, 045205 (2012).

[53] A. Bashir, L. Chang, I. C. Cloet, B. El-Bennich, Y. -X. Liu, C. D. Roberts and P. C. Tandy, Commun. Theor. Phys. **58**, 79 (2012).

[54] K. -I. Kondo, K. Suzuki, H. Fukamachi, S. Nishino and T. Shinohara, arXiv:1209.3994 [hep-th].

[55] S. Strauss, C. S. Fischer and C. Kellermann, arXiv:1208.6239 [hep-ph].

[56] J. S. Ball and T. W. Chiu, Phys. Rev. D **22**, 2550 (1980) [Erratum-ibid. D **23**, 3085 (1981)].

[57] A. C. Aguilar, D. Binosi, J. Papavassiliou and J. Rodriguez-Quintero, Phys. Rev. D **80** (2009) 085018.

[58] C. H. Llewellyn-Smith, Annals Phys. **53** (1969) 521.

[59] P. Maris and C. D. Roberts, Int. J. Mod. Phys. E **12** (2003) 297.

[60] J. D. Bjorken and S. D. Drell, "Relativistic Quantum Field Theory", McGraw-Hill Inc (1965), chapter 19.

[61] P. Pascual and R. Tarrach, "Qcd: Renormalization For The Practitioner," Lect. Notes Phys. **194**, 1 (1984).

[62] A. I. Davydychev, P. Osland and O. V. Tarasov, Phys. Rev. D **54**, 4087 (1996) [Erratum-ibid. D **59**, 109901 (1999)].

[63] P. A. Grassi, T. Hurth and A. Quadri, Phys. Rev. D **70** (2004) 105014.

[64] A. C. Aguilar, D. Binosi and J. Papavassiliou, JHEP **0911** (2009) 066.

[65] A. C. Aguilar, D. Binosi and J. Papavassiliou, JHEP **1007** (2010) 002.

[66] D. Ibanez, PoS QCD **-TNT-II**, 025 (2011).

[67] D. Binosi and J. Papavassiliou, JHEP **1103** (2011) 121.

[68] J. M. Cornwall and W. -S. Hou, Phys. Rev. D **34**, 585 (1986).

[69] A. Cucchieri, A. Maas and T. Mendes, Phys. Rev. D **74**, 014503 (2006).

[70] A. Cucchieri, T. Mendes, G. M. Nakamura and E. M. S. Santos, PoS FACESQCD , 026 (2010).

[71] A. Cucchieri, T. Mendes, G. M. Nakamura and E. M. S. Santos, AIP Conf. Proc. **1354**, 45 (2011).

[72] D. Binosi and A. Quadri, Phys. Rev. D **85**, 121702 (2012).

[73] A. Cucchieri and T. Mendes, Phys. Rev. D **86**, 071503 (2012).